Journal Pre-proof

Design, synthesis and biological activity of novel 2,3,4,5-tetra-substituted thiophene derivatives as PI3Kα inhibitors with potent antitumor activity

Weike Liao, Zhongyuan Wang, Yufei Han, Yinliang Qi, Jiaan Liu, Juan Xie, Ye Tian, Qiancheng Lei, Rui Chen, Ming Sun, Lei Tang, Guowei Gong, Yanfang Zhao

PII: S0223-5234(20)30278-6

DOI: https://doi.org/10.1016/j.ejmech.2020.112309

Reference: EJMECH 112309

To appear in: *European Journal of Medicinal Chemistry*

Received Date: 3 January 2020

Revised Date: 1 April 2020

Accepted Date: 2 April 2020

Please cite this article as: W. Liao, Z. Wang, Y. Han, Y. Qi, J. Liu, J. Xie, Y. Tian, Q. Lei, R. Chen, M. Sun, L. Tang, G. Gong, Y. Zhao, Design, synthesis and biological activity of novel 2,3,4,5-tetra-substituted thiophene derivatives as PI3Kα inhibitors with potent antitumor activity, *European Journal of Medicinal Chemistry* (2020), doi: https://doi.org/10.1016/j.ejmech.2020.112309.

Graphical Abstract

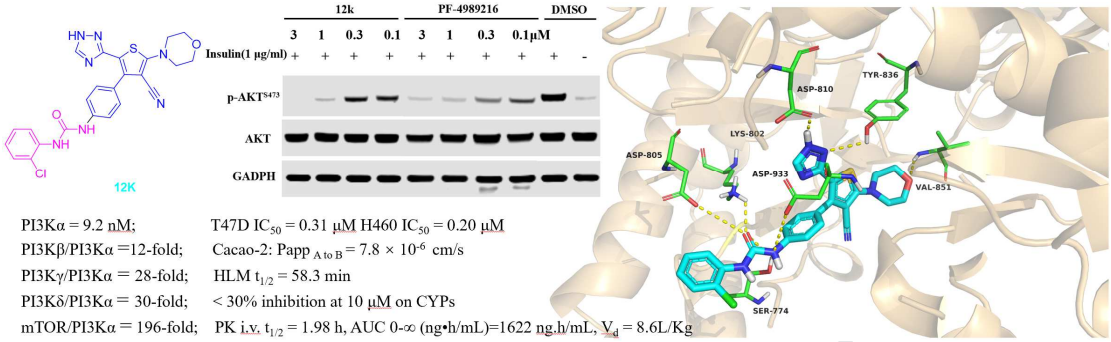

PI3Kα = 9.2 nM; T47D IC_{50} = 0.31 μM H460 IC_{50} = 0.20 μM
PI3Kβ/PI3Kα =12-fold; Cacao-2: $Papp_{A\ to\ B}$ = 7.8 × 10^{-6} cm/s
PI3Kγ/PI3Kα = 28-fold; HLM $t_{1/2}$ = 58.3 min
PI3Kδ/PI3Kα = 30-fold; < 30% inhibition at 10 μM on CYPs
mTOR/PI3Kα = 196-fold; PK i.v. $t_{1/2}$ = 1.98 h, AUC 0-∞ (ng•h/mL)=1622 ng.h/mL, V_d = 8.6L/Kg

Two series of novel 2,3,4,5-tetra-substituted thiophene derivatives containing diaryl urea or *N*-Acylarylhydrazone scaffold were designed and synthesized to evaluate their anticancer activities

Design, synthesis and biological activity of novel 2,3,4,5-tetra-substituted thiophene derivatives as PI3Kα inhibitors with potent antitumor activity

Weike Liao[a,1], Zhongyuan Wang[b,1], Yufei Han[c,1], Yinliang Qi[c], Jiaan Liu[e], Juan Xie[b], Ye Tian[c], Qiancheng Lei[a], Rui Chen[a], Ming Sun[c], Lei Tang[a***], Guowei Gong[d**], Yanfang Zhao[c*]

[a] *State Key Laboratory of Functions and Applications of Medicinal Plants, Guizhou Provincial Engineering Technology Research Center for Chemical Drug R&D, Guizhou Medical University, Guiyang 550004, PR China.*

[b] *Department of Pharmacy, Guizhou Provincial People's Hospital, Guiyang 550002, PR China.*

[c] *Key Laboratory of Structure-Based Drug Design and Discovery (Shenyang Pharmaceutical University), Ministry of Education, 103 Wenhua Road, Shenhe District, Shenyang 110016, PR China*

[d] *Department of Bioengineering, Zunyi Medical University, Zhuhai Campus, Zhuhai 519041, Guangdong, PR China*

[e] *Department of Chemistry, University of Massachusetts-Amherst, Massachusetts 01003, United States*

Abstract

Using a rational design strategy for isoform-selective inhibition of PI3Kα, two series of novel 2,3,4,5-tetra-substituted thiophene derivatives containing either diaryl urea or N-Acylarylhydrazone scaffold were designed and synthesized. The most promising compound **12k** was demonstrated to bear nanomolar PI3Kα inhibitory potency with 12, 28, 30, 196-fold selectivity against isoforms β, γ, δ and mTOR. Besides, it also showed good developability profiles in cell-based proliferation against a panel of human tumor cells as well as ADME assays. We herein report on their design, synthesis, SAR and potential developability properties.

Keywords: PI3Kα; antiproliferative activities; synthesis; 2,3,4,5-tetra-substituted thiophene derivatives

1. Introduction

Phosphatidylinositol-3-kinases (PI3Ks) play a distinctly important role in a variety of downstream effectors mediating cellular processes, including cell growth, proliferation, survival, and differentiation.[1-4] According to sequence homology and substrate preference, PI3Ks can be classified into classes I, II and III.[5] The PI3K family in class I consists of four isoforms (α, β, γ, and δ). Recently, activated PI3Kα, β, and δ signaling pathway has been increasingly related to cancer, and these isoforms can be activated by inactivation of the tumor suppressor PTEN[6-8] and direct somatic mutations in PIK3CA which encodes the p110α subunit of PI3K.[9] The human

* Corresponding author.
** Corresponding author.
*** Corresponding author.
E-mail addresses: tlei1974@hotmail.com (L. Tang), sammyld@163.com (G. Gong), yanfangzhao@126.com (Y. Zhao).
[1] These authors contributed equally to this work.

tumor genetic data indicated that mutations in PI3Kα can prompt tumor growth.[10] Furthermore, a selective inhibitor that does not bind to PI3Kβ, δ, and γ may reduce some treatment side effects caused by preventing platelet aggregation and activation,[11] inhibiting immune responses mediated by T, B, and mast cells, [12] and blocking anti-inflammatory signals, [13] *etc*. Giving these observations, targeting PI3Kα pathway will be one of the most promising approaches for cancer treatment.

Recently, notable success for PI3K-isoform selective inhibitors had been achieved, Idelalisib (**1**) [14,15], previously called GS-1101 or CAL-101, was a first-in-class, oral, potent, and selective inhibitor of PI3Kδ. Also, Alpelisib[16,17](**2**), a selective PI3Kα inhibitor was approved by the FDA on May 24, 2019, in Combination With Fulvestrant for patients with HR+, HER2-, PIK3CA-mutated advanced breast cancer. Furthermore, several class I selective PI3K inhibitors were in various phases of clinical trials, including PF-4989216 (**3**),[18] and GDC-0032 (**4**)[19,20] for PI3Kα/δ and AZD8186 (**5**)[21] for PI3Kβ (**Fig. 1**). Among them, PF-4989216 exhibited potent and selective inhibition against PI3K kinase activity in preclinical small-cell lung cancer (SCLC) models and was especially effective against the proliferation of SCLCs harboring PIK3CA mutation. Among all four isoforms of PI3K, the importance and high frequency of PIK3CA mutation in most of the solid tumors aroused the concern about the selectivity development of PI3Kα inhibitors. [22] Present work aims to design, synthesize, and optimize 2,3,4,5-tetra-substituted thiophene derivatives, which can selectively bind to PI3Kα ATP binding site.

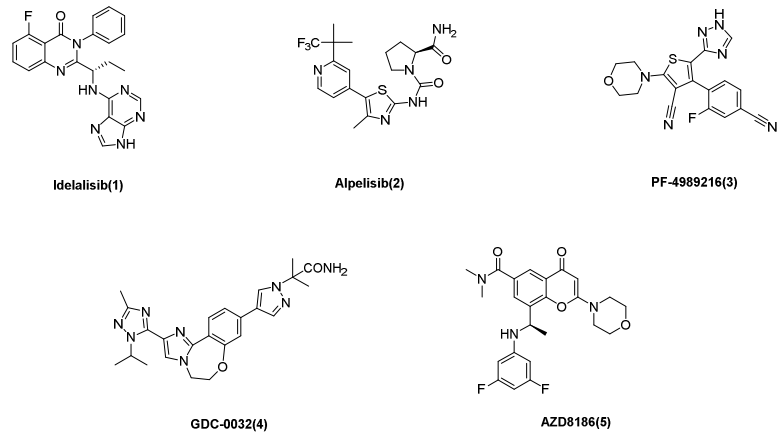

Fig.1. Representative Structures of PI3K inhibitor

From the docking model of PF-4989216 with PI3Kα protein (PDB code 3ZIM),[23] the key

hydrogen-bonding interactions were formed by the 1,2,4-triazole moiety and the morpholino group with residues in the ATP binding site (**Fig. 2)**. Through a detailed docking analysis, C-4 phenyl moiety did not generate any hydrogen-bonding interactions with the residues directly or indirectly. Therefore, appropriate groups in C-4 phenyl moiety were introduced to explore potential interactions with the residues in solvent zone in order to increase PI3Kα selectivity. In our previous study, it was observed that the small molecules bearing the diaryl urea scaffold or *N*-Acylarylhydrazone moiety showed superior anticancer activity due to the presence of hydrogen bond donors and acceptors as well as its flexible skeleton.[24, 25] Based on these findings, the diaryl urea scaffold or *N*-Acylarylhydrazone moiety was introduced into C-4 phenyl moiety on PF-4989216. As a result，two series of novel 2,3,4,5-tetra-substituted thiophene derivatives were designed and synthesized. Compounds were screened for their PI3K/mTOR inhibitory activity and cytotoxicity in a panel of cancer cell lines. Additionally, in Vitro ADME and Pharmacokinetics, data for compound **12k** was also investigated.

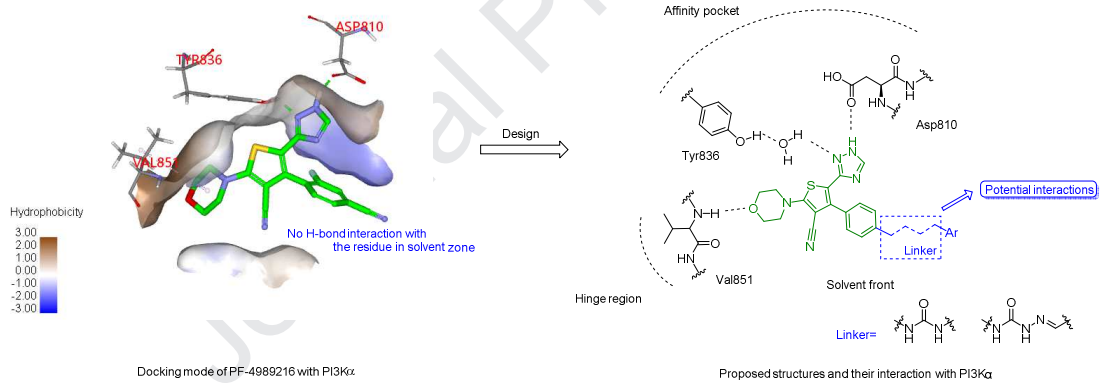

Fig. 2 The design strategy based on the docking study

2. Results and discussion

2.1. Chemistry

The general synthetic routes of the title compounds are illustrated in **Schemes 1–3**. The key intermediate 2,3,4,5-tetrasubstituted thiophene **11** was achieved in 11 steps as shown in **Scheme 1**. Commercially available malononitrile was condensed with carbon disulfide in the presence of K_2CO_3 in DMSO at 0-20 ºC for 2 h to obtain 2-(dimercaptomethylene)malononitrile, followed by methylated with iodomethane at 20 ºC for another 20 h to provide 2-(bis(methylthio)methylene)malononitrile **1**. Further, intermediate **1** was treated with ethyl

2-mercaptoacetate to generate ethyl 3-amino-4-cyano-5-(methylthio)thiophene-2-carboxylate (**2**) [26], which was then iodinated in the presence of isoamyl nitrite in acetonitrile to yield intermediate **3**. Oxidation of intermediate **3** with 30% H_2O_2 and sodium tungstate in acetic acid gave ethyl 4-cyano-3-iodo-5-(methylsulfonyl)thiophene-2-carboxylate(**4**), which was reacted with morpholine through an S_N2 mechanism to generate intermediate **5**. Subsequently, intermediate **5** was subjected to palladium-catalyzed Suzuki-coupling reaction with 4-(*N*-Boc-amino)phenylboronic acid pinacol ester in hot dioxane/toluene/H_2O (16:1:4, 95 ºC) to get a key intermediate **6**, which was hydrolyzed to acid **7** by aqueous LiOH in MeOH:THF (1:2). Treatment of **7** with methyl chloroformate in the presence of Et_3N yielded anhydride intermediate, which was converted to tert-butyl (4-(2-carbamoyl-4-cyano-5-morpholinothiophen-3-yl)phenyl)carbamate **8** by ammonium hydroxide. Then, **8** was condensed with *N*,*N*-dimethylformamide dimethyl acetal (DMF-DMA) at 110 ºC for 2 h to afford **9**, which was treated with hydrazine hydrate in acetic acid at 60 ºC for 2 h to give intermediate **10.** The key intermediate 2,3,4,5-tetrasubstituted thiophene **11** was obtained by the deprotection of **10** in the presence of trifluoroacetic acid in CH_2Cl_2 at room temperature for 3 h.

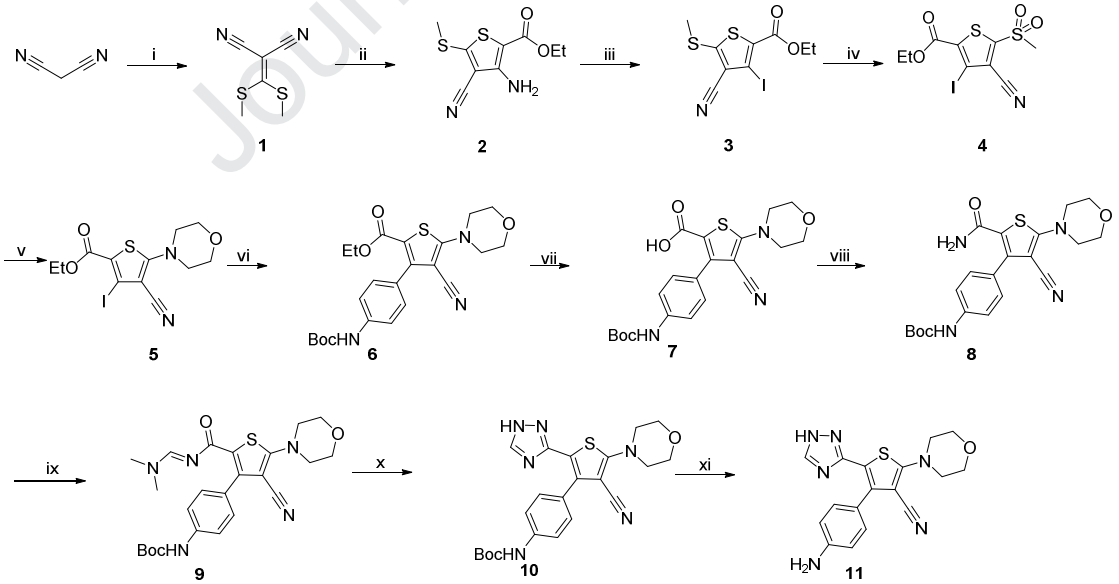

Scheme 1. Reagents and conditions: (i) a) CS_2, K_2CO_3, DMSO, 20 ºC, 2 h; b) iodomethane, 20 ºC, 12 h; (ii) ethyl 2-mercaptoacetate, Et_3N, EtOH, 20 ºC, 12 h; (iii) isoamyl nitrite, I_2, CH_3CN, 20 ºC, 12 h; (iv) 30% H_2O_2, sodium tungstate, HOAc, 60 ºC, 2 h; (v) morpholine, THF, r.t., 8 h; (vi) a) 4-(*N*-Boc-amino)phenylboronic acid pinacol

ester, CsF, 1,4-dioxane:H_2O (4:1), r.t., 15 min; b) $Pd_2(dba)_3$, $P(t\text{-}Bu)_3$, Toluene/dioxane, 95 ºC, 12 h; (vii) LiOH, MeOH:THF (1:2), r.t., 4 h; (viii) a) methyl chloroformate, Et_3N, THF, r.t., 3 h; b) $NH_3 \cdot H_2O$, r.t., 1 h; (ix) DMF-DMA, DMF, 110 ºC, 2 h; (x) hydrazine hydrate, HOAc, 60 °C, 2 h; (xi) CF_3COOH, CH_2Cl_2, r.t., 3 h.

The target compounds **12a-m** were prepared, as illustrated in **Scheme 2.** The commercially available substituted isocyanatobenzene was treated with the key intermediate **11** in CH_2Cl_2 at room temperature for 12 h to afford the target compounds **12a-m**.

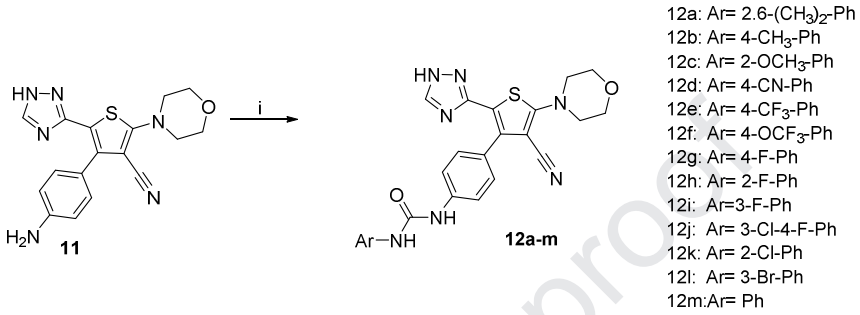

Scheme 2. Reagents and conditions: (i) isocyanatobenzene, CH_2Cl_2, r.t., 12 h.

As described in **Scheme 3,** the key intermediate **11** was converted into amides **13** by the treatment with phenyl chloroformate in dry acetone at ambient temperature for 3 h; subsequently, hydrazinolysis of **13** with 80% hydrazine hydrate in refluxing 1,4-dioxane for 2 h provided semicarbazide **14**, followed by condensation with appropriate aldehydes in EtOH at 80 °C for 5 h with catalytic amount of acetic acid to give the target compounds **15a-m** successfully.

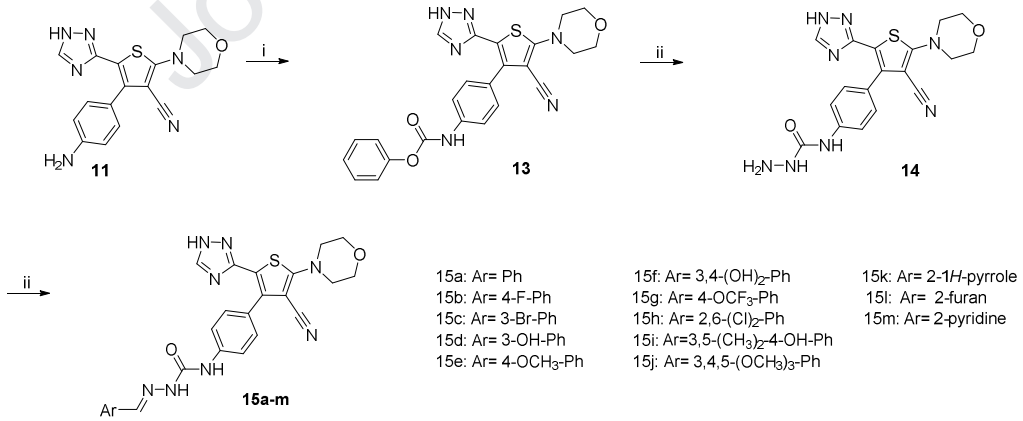

Scheme 3. Reagents and conditions: (i) phenyl chloroformate, dry acetone, r.t., 3 h.; (ii) 80% hydrazine hydrate, 1,4-dioxane, reflux, 2 h; (iii) aldehydes, acetic acid, EtOH, 80 °C, 5 h.

The chemical structures of the target compounds were confirmed with ^{1}H NMR, ^{13}C NMR, and MS spectrum. Also, the configuration of the double bond in the imine of **15a-m** was determined. In ^{1}H NMR spectra, the –N=C***H***- signal was observed as a single peak for each

compound, indicating that only one isomer was generated. To confirm the stereochemistry more accurately, the NOESY experiment of compound **15d** was performed. The result showed that a single NOE signal was observed between the proton of =N-N***H***- (δ = 10.80 ppm) and the proton of –N=C***H***- (δ = 8.46 ppm), which existed only in the *E* isomer due to the appropriate intramolecular H-H distance (**Fig.3.** and see also Supporting information). Thus, the target compounds were unequivocally confirmed as the *E* isomer.

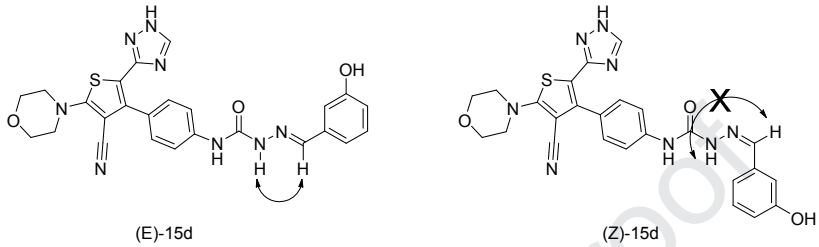

Fig. 3. NOESY effect of the representative compound **15d.**

2.2. Bioactivity and discussion

2.2.1. PI3K/mTOR inhibition and SAR study of target compounds

During the course of our SAR investigation, compound **12m** with diaryl urea scaffold was firstly synthesized and evaluated. We found compound **12m** exhibited an IC_{50} of 116 nM in PI3Kα assay (**Table 1**), which was around 21-fold less potent compared to PF-4989216. Next, we assembled a focused collection of diaryl urea analogues that could be readily synthesized; the effect of substitute group at the 4-position was first assessed. Introduction of electron-donating group such as -CH_3, -OCH_3 did not offer the potency benefit (**12a** to **12c** vs **12a**). A strong electron-withdrawing group such as -CN, -CF_3, -OCF_3 proved to be deleterious to PI3Kα potency, as a gradual decrease in potency was observed (**12d** to **12f** vs **12a**). However, when the small electron-withdrawing fluoride group was introduced, compound **12g** gained back some degree of potency (3.8-fold increase vs **12a**) but still around 6-fold less potent than PF-4989216. Through scanning the 2-, 3-position of phenyl, it was clearly found that 3-position was not well tolerated (**12i** vs **12g**); a similar trend was also observed for compound **12j** (**12j** vs **12g**), whereas ortho-fluoro substitute compound **12h** showed slightly enhanced PI3Kα activity. Further replacement of fluoro with the chloro group led to isolation of the potent PI3Kα inhibitor **12k** with an IC_{50} of 9.2 nM. These data suggested that a proper degree of electron density on the terminal aromatic ring was beneficial to achieve better inhibitory activity.

In comparison, the SARs of compounds **15a-m** bearing *N*-Acylarylhydrazone moiety were conducted in the same way. Compound **15a** maintained a PI3Kα inhibitive activity similar to that of **12a**. We found phenyl substitution such as halogen (**15b**, **15c**) did not have a profound impact on PI3Kα potency. However, a noticeable improvement was seen with a hydroxyl group at the 3-position (**15d** vs **15a**). Meanwhile, it was also noted that introduction of a 3,4-dihydroxy **15f** or 3,5-dimethyl-4-hydroxy group **15i** led to a similar potency improvement as **15d**. In contrast, the introduction of electron-withdrawing trifluoromethoxy group eroded the PI3Kα potency (**15g** vs. **15a**). With SAR expansion, analogs with six or five-membered heterocycles (**15k** to **15m**) were also prepared. Notably, compound **15m**, which exhibited an IC_{50} of 6.9 nM against PI3Kα, had been optimized up to the similarly level of PF-4989216.

Table 1. SAR studies of compounds **12a-m** and **15a-m**

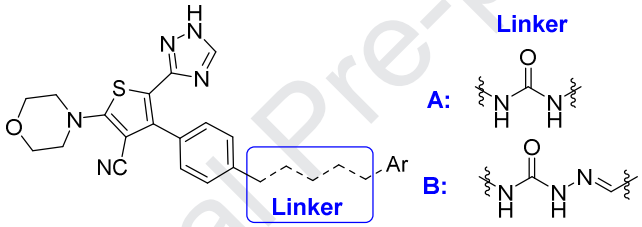

Compd.	Linker	Ar	PI3Kα IC_{50}(nM)[a]	Compd.	Linker	Ar	PI3Kα IC_{50}(nM)[a]
12a	A	2.6-$(CH_3)_2$-Ph	344	**15a**	B	Ph	76.6
12b	A	4-CH_3-Ph	95.8	**15b**	B	4-F-Ph	75.5
12c	A	2-OCH_3-Ph	105	**15c**	B	3-Br-Ph	89.8
12d	A	4-CN-Ph	290	**15d**	B	3-OH-Ph	17.7
12e	A	4-CF_3-Ph	403	**15e**	B	4-OCH_3-Ph	72.0
12f	A	4-OCF_3-Ph	835	**15f**	B	3,4-$(OH)_2$-Ph	21.9
12g	A	4-F-Ph	35.3	**15g**	B	4-OCF_3-Ph	631
12h	A	2-F-Ph	22.3	**15h**	B	2,6-$(Cl)_2$-Ph	323

12i	A	3-F-Ph	151	**15i**	B	3,5-$(CH_3)_2$-4-OH-Ph	20.3
12j	A	3-Cl-4-F-Ph	407	**15j**	B	3,4,5-$(OCH_3)_3$-Ph	110
12k	A	2-Cl-Ph	9.2	**15k**	B		9.4
12l	A	3-Br-Ph	239	**15l**	B		13.3
12m	A	Ph	116	**15m**	B		6.5
	PF-4989216[b]		5.4	**BYL-719(Alpelisib)**[b]			3.9

[a] The average is indicated ($n \geq 2$ independent experiments); [b] Used as a positive control.

Through the SAR investigation, novel thiophene derivatives were identified to bear decent potency against PI3Kα. Six representative compounds were selected for further profiling. The inhibitory activities to other Class I PI3K isoforms (β, γ, and δ) and mTOR were evaluated. As show in **Table 2**, all the tested compounds displayed more potent activity against PI3Kα than the rest of three isoforms as well as mTOR. Additionally, compounds (**12g**, **12h**, **12k**) bearing diaryl urea moiety displayed a higher level of selectivity than that of compounds with *N*-Acylarylhydrazone scaffold, especially towards PI3Kδ and mTOR, making it a promising selective PI3Kα inhibitor. We believed that the overall profiles obtained from the enzyme assays would contribute significantly to the further design of more potent and selective inhibitors.

Table 2. Inhibitory effects of compounds and **PF-4989216**, **BYL-719** against PI3Ks and mTOR

Compound	IC_{50} in nM[a]			
	PI3Kβ	PI3Kγ	PI3Kδ	mTOR
12g	95	289	238	1662
12h	89	302	334	1589
12k	108	258	275	1802
15d	43	440	72	489
15l	74	204	74	598
15m	53	274	49	416
PF-4989216 [b]	124	60	15	4064
BYL-719(Alpelisib)[b]	1540	94	72	1461

[a] Data reported as the average of at least two runs; [b] Used as a positive control.

2.2.2. In vitro Antiproliferative Activity

To investigate the functional consequence of inhibiting PI3Kα in cells, compounds were also tested in five different cancer cell lines for its sensitivity in cell proliferation assays. Cell lines either harbor PIK3CA mutations or bear the PTEN deletion except for A549 were treated, and growth was monitored. Interestingly, these selective PI3K inhibitors were more sensitive with human breast cancer and non-small cell lung cancer cell lines that harbor PI3KCA mutations than cell lines with the PTEN deletion, as shown in **Table 3**. Consistent with the potency against the PI3K, compound **12g**, **12h**, **12k** were moderately potent with at least single-digital micromolar IC_{50}s across tumor cell originating from different tissues. Notably, compound **12k** potently inhibited the proliferation of human breast cancer line T47D and human lung adenocarcinoma NCI-H460 with IC_{50} of 0.31 and 0.20 μM, respectively. However, an apparent disconnection between the cell activity and the PI3Kα inhibition of compounds **15d**, **15l**, **15m** was observed. The *N*-Acylarylhydrazone analogs are active in the PI3K assay but possess weak cytotoxicity in cells probably due to their low membrane permeability. In view of this, compound **12k** was selected for further profiling.

Table 3. Antiproliferative Effect of Compounds against a Panel of Human Cancer Cell

	IC_{50} in μM[a]				
Compound	**U87MG[c]**	**T47D[d]**	**NCI-H1975[d]**	**NCI-H460[d]**	**A549[e]**
12g	3.35	0.52	2.04	0.59	5.52
12h	3.98	0.41	1.52	0.40	4.19
12k	2.86	0.31	1.06	0.20	3.84
15d	13.01	2.22	9.76	1.39	12.66
15l	12.29	2.68	12.89	1.22	19.36
15m	22.14	2.13	11.20	2.69	18.52
PF-4989216 [b]	2.31	0.34	0.94	0.12	3.58

[a] Cell viability was measured using a CellTiter-Glo assay 72 h after treatment. Average IC_{50} values (n = 3) are

shown. [b] Used as a positive control. [c] Tumor cell line with PTEN deletion. [d] Tumor cell line harboring PIK3CA mutation. [e] Tumor cell line harboring neither PIK3CA mutation nor PTEN deletion.

*2.2.3. Kinase selectivity profiling of **12k***

Given the fact that **12k** exhibited the desirable in vitro biochemical activity against PI3Ks as well as antiproliferative efficacy in cancer cell lines, **12k** was further chosen to examine its kinome wide selectivity profile containing 97 kinases (scanEDGE KINOMEscan, DiscoverX) at a compound concentration of 1 μM. **12k** proved to be highly selective as **PF-4989216** against the panel, compound **12k** did not show any binding activity to this broad panel of kinases except for the PI3Ks, illustrating excellent kinase selectivity for this thiophene chemotype. The results are shown in **Figure 4** and the complete profiling data of **12k** and **PF-4989216** on 97 kinases can be found in Table S2 of the Supporting Information.

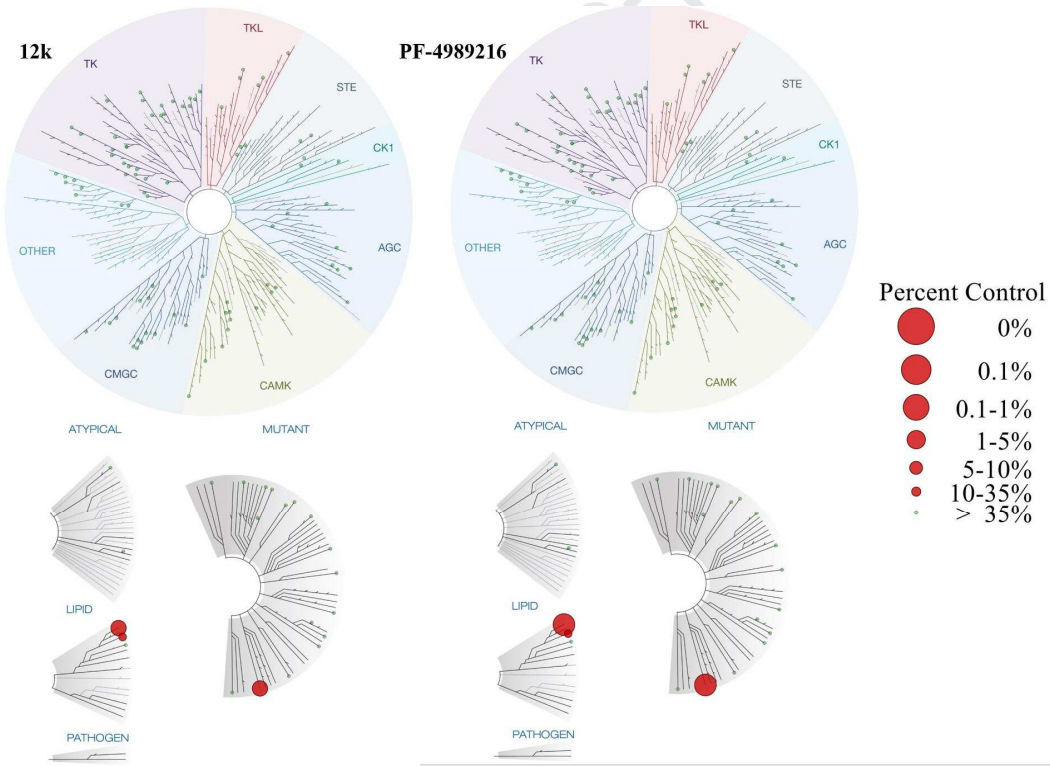

Fig. 4. Percent inhibition profile (TREEspot Interaction Map) in the DiscoverX ScanEDGE kinome scan for compound **12k** and **PF-4989216. S**-score is a quantitative measure of compound selectivity. It is calculated by dividing the number of kinases that compounds bind to by the total number of distinct kinases tested, excluding mutant variants.

2.2.4. Western Blot

Activation of the PI3K pathway leads to phosphorylation of the Ser^{473} of Akt and subsequently to several downstream substrates. To confirm that the newly synthesized compounds were inhibiting PI3K signaling in cells, **12k** was further profiled for its ability to suppress cellular biomarkers. After treatment with **12k** for 2 h, T47D cells were treated with 1 μg/mL insulin to activate the PI3K pathway. Consistent with expectations for a potent PI3Kα inhibitor, **12k** strongly suppressed phosphorylation of Akt at the serine 473 in a dose dependent manner. We also compared the suppression of PI3K signaling by **12k** with **PF-4989216**, as shown in **Figure 5**. Compound **12k** shows p-Akt reduction starting at 0.1 μM and is complete at 3 μM. We concluded that the anti-proliferative activity of **12k** against T47D cell line was attributed to its remarkable capability to attenuate the PI3K signaling.

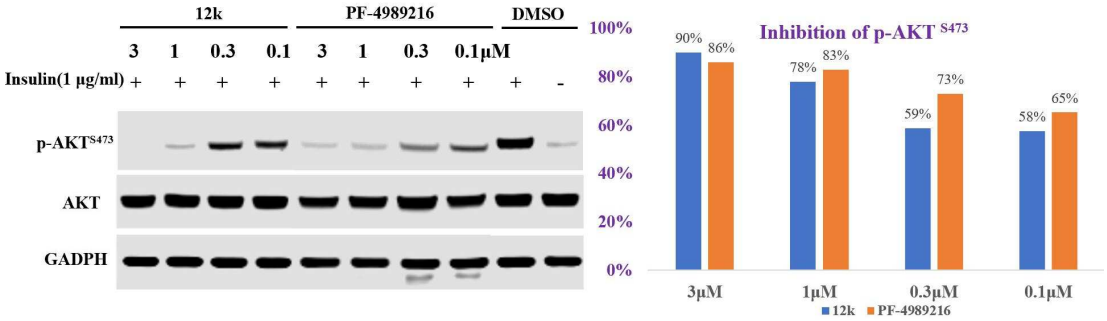

Fig. 5. Effects of **12k** and **PF-4989216** on p-Akt^{S373}, Akt. T47D cells were treated with various concentration of **12k** or **PF-4989216** for 2 h, and then the PI3K pathway was activated by treatment of 1 μg/mL insulin for 2 h. Compound **12k** decreased the phosphorylation of Akt^{S473} in a dose-dependent manner.

*2.2.5. In Vitro ADME and Pharmacokinetics for Compound **12k***

In vitro ADME properties and pharmacokinetic parameters of compound **12k** were also determined. Caco-2 bidirectional permeability assay confirmed that **12k** had moderate permeability and was not a substrate for P-glycoprotein (efflux ratio of 1.08). From the multispecies liver microsomal stability study, compound **12k** showed acceptable stability with clearance rate of 24.8, 32.8 μL/min/mg in human and rat liver microsomes, respectively. Also, three cytochrome P450 (CYP1A2, 2D6 and 3A4) enzymes commonly metabolizing exogenous chemicals were used to test the direct inhibition of compound **12k**. As listed in **Table 4**, the compound showed favorable metabolic properties, as the inhibition ratio for three CYPs was less than 30%, even at the concentration of 10 μM. With these in vitro effects and preliminary ADMET profiling, further intravenous pharmacokinetic parameters for **12k** were performed by

Sprague−Dawley rats at a dose of 5 mg/kg, **12k** exhibited a moderate half-life of 1.98 ± 0.17 h and achieved a maximum concentration (C_{max}) of 2.57 ± 0.32 μg/mL. The area under the curve (AUC(0−∞)) was 1622 ± 89 ng·h/mL. It is worth noting that compound **12k** exhibited relatively high plasma clearance (52.36 ± 3.32 mL/min/kg). Finally, compound **12k** was found to be safe (IC_{50} > 30 μM, see **Fig. S2**) when tested in a hERG Qpatch assay for assessing hERG-associated cardiotoxicity.

Table 4. In Vitro ADME and Pharmacokinetics for Compound **12k**

Permeability assay (10^{-6} cm/s) [a]			
Caco-2	Papp (A to B)	Papp (B to A)	Efflux ratio
-	7.8	8.4	1.08
Metabolic stability [b]			
Species	$T_{1/2}$(min)	CL (μL/min/mg)	Remaining [b] (T=60min)
RLM	44.7	32.8	42.6%
HLM	58.3	24.8	47.8%
CYP450 inhibition [c]			
isozyme	CYP1A2	CYP2D6	CYP3A4
% inhibition at 10μM	27.8	28	1.5
Pharmacokinetics [d]			
C_{max}(μg/mL)	$t_{1/2}$ (h)	V_d (L/Kg)	CL (mL/min/kg)	AUC 0-∞ (ng•h/mL)
2.57±0.32	1.98±0.17	8.6±1.33	52.36±3.32	1622±89

[a]The permeation was assessed over 2 h with 2 μM concentration incubation at 37±1°C and 5% CO_2 with saturated humidity. [b] No NADPH regenerating system was added to the sample (replaced by buffer) during the 60 min incubation. [c] Performed at 10 μM concentration. α-Naphthoflavone (CYP1A2), squinidine (CYP2D6), and ketoconazole (CYP3A4) were used as the positive controls. [d] Determined from intravenous dosing to male SD rats at a dose of 5 mg/kg (n=6).

2.2.6. Binding model analysis

The better understand the isoform selectivity of **12k** against PI3Ks, the affinity of compound **12k** for each PI3K isoform was calculated by applying the Cheng-Prusoff equation. Compound **12k** exhibited Ki values of 5.1nM, 89 nM, 193 nM, 245 nM against PI3Kα, PI3Kβ, PI3Kγ, PI3Kδ, respectively (see Table S1 for details). The binding modes between the **12k** and PI3Ks were then proposed by molecular simulation. The structures of PI3Kα (PDB ID code: 3ZIM), PI3Kβ (PDB ID code: 2Y3A), PI3Kγ (PDB ID code: 3DBS) and PI3Kδ (PDB ID code: 2WXP) were selected as the docking models.

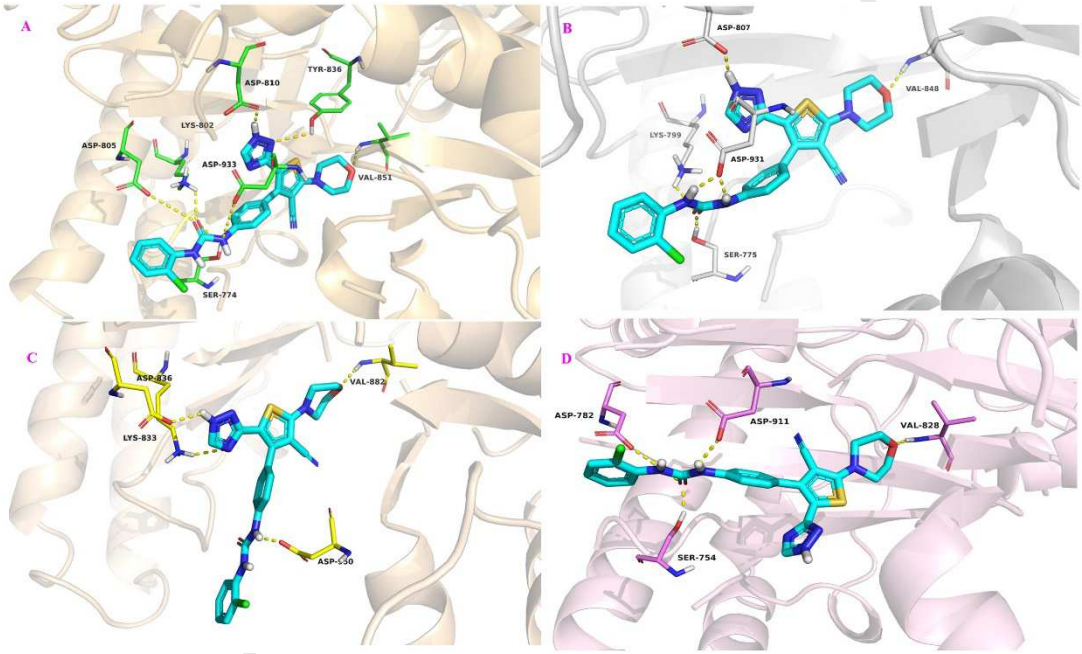

Fig. 6. Predicted binding models for **12k** with PI3Ks. (A) Predicted binding conformation for **12k** in the binding site cavity of PI3Kα (PDB 3ZIM). (B) Binding to PI3Kβ (PDB 2Y3A). (C) Binding to PI3Kγ (PDB 3DBS). (d) Binding to PI3Kδ (PDB 2WXP). Hydrogen bonds are indicated by yellow dashed lines. Images generated using PyMol.

As shown in **Fig. 6A**, compound **12k** occupied the kinase domain in a similar manner to PF-4989216. Six hydrogen-bond interacted with **12k** and PI3Kα: the morpholine moiety formed one hydrogen bond with Val 851; meanwhile, the 1,2,4-triazole group formed two hydrogen bonds with Tyr 863 and Asp 810. Besides, the urea part of compound **12k** could form three hydrogen bonds with Asp 805, Asp 933 and Ser 774, validating the rationality of our design. We also performed the docking analysis of compound **12k** binding to β (PDB 2Y3A) (**Fig. 6B**) and γ (PDB 3DBS) (**Fig. 6C**) isoforms. Six hydrogen-bond interactions with residues of PI3Kβ were noticed:

Val 848, Asp 807, Asp 931, Lys 799 and Ser 775. For the binding of **12k** to PI3Kγ, four hydrogen-bond interactions with the residues were indicated: Val 882, Asp 836, Asp 950 and Lys 833. The analysis of compound **12k** with PI3Kδ showed that this compound formed four hydrogen-bond interactions with Val 828, Asp 911, Asp 782 and Ser 754. Also, compound **12k** was in a reversed pose in PI3Kδ compared to PF-4989216 (**Fig. 7**), which indicated compound **12k** could not fit well into the cavity of PI3Kδ isoform, thus resulted in a decrease of inhibitory activity against PI3Kδ. Furthermore, molecular dynamics calculations had been implemented to verify the stability of ligand-protein complexes in the proposed model. The MD simulation undertaken for the two compounds bound to PI3Kδ showed the overall stability of the ligand/target adducts over the tested 25 ns (see **Fig. S3**). In general, the docking results further confirm the rationality of our design strategy.

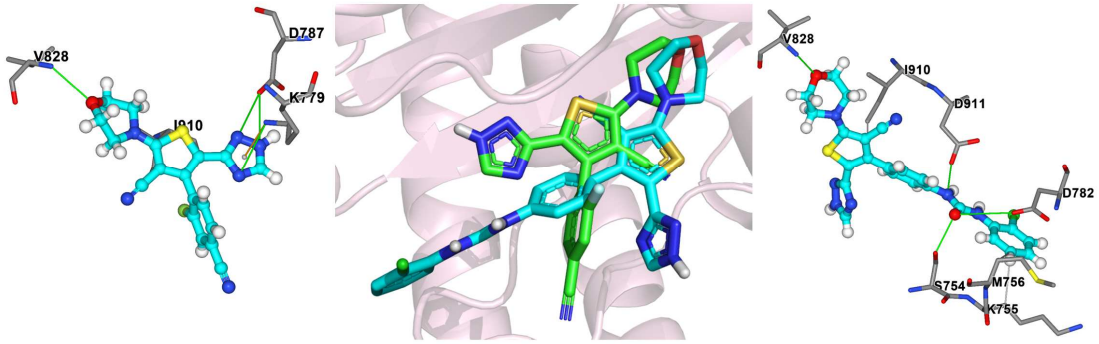

Fig 7. Overlapping images of compound 12k (blue) and PF-4989216(green) complexed with PI3Kδ. Hydrogen bonds are indicated by blue lines.

3. Conclusions

In this study, two series of novel potent PI3Kα inhibitors bearing the diaryl urea scaffold or *N*-Acylarylhydrazone moiety based on PF-4989216 were designed. The PI3K enzymatic activity assays identified compound **12k** as a selective PI3Kα inhibitor with 12, 28, 30, 196-fold selectivity over isoforms β, γ, δ and mTOR. Compound **12k** also showed potent cytotoxic activities with IC_{50} values of 0.31 μM and 0.20 μM against human breast cancer T47D and non-small cell lung cancer H460 cell lines, respectively. To evaluate its druggability, compound **12k** was submitted to in vitro ADME and in vivo Pharmacokinetics assay. The pharmacokinetic properties of the compound **12k** are suboptimal and are the focus of a medicinal chemistry e ·ort to improve its oral bioavailability while maintaining its potency and selectivity. This will be the focus of a future publication.

4. Experimental

4.1. Chemistry

Unless otherwise specified, reagents and solvents were obtained from commercial sources and used without further purification. Reactions' time and purity of the products were monitored by TLC on FLUKA silica gel aluminum cards (0.2 mm thickness) with fluorescent indicator 254 nm. All melting points were obtained on a Büchi Melting Point B-540 apparatus (Büchi Labortechnik, Flawil, Switzerland) and were uncorrected. Flash chromatography was performed using silica gel (200–300 mesh) from Qingdao ocean Chemicals (Qingdao, Shandong, China). PF-4989216 and BYL-719 were purchased from TargetMol (Shanghai, China). Mass spectra (MS) were taken in ESI mode on Waters e2695. ^{1}H NMR and ^{13}C NMR spectra were recorded on Bruker ARX-400, 400 MHz spectrometers (Bruker Bioscience, Billerica, MA, USA) with TMS as an internal standard.

*4.2. Synthesis of the key intermediate **11***

*4.2.1. Preparation of 2-(bis(methylthio)methylene)malononitrile(**1**)*

A suspension of K_2CO_3 (17.3 g, 125.0 mmol) in DMSO (75 mL) at 20 °C was treated with malononitrile (7.5 g, 113.7 mmol) in one portion. The reactor was cooled to 0 °C, and CS_2 (7.5 mL, 125.0 mmol) was added at 18-22 °C. The mixture was stirred at 20 °C for 2 h and then cooled to 0 °C. Iodomethane (14.1 mL, 227.3 mmol) was added with pot temperature below 5 °C. The reaction was warmed to 20 °C and stirred for 12 h. The reaction mixture was poured into ice-water (75 mL), and the resulting precipitate was filtered, washed with H_2O (20 mL) and dried under reduced pressure to afford product **1** as a yellow solid (18.2 g, 93.9%). ^{1}H NMR (400 MHz, $CDCl_3$) δ 2.69 (s, 6H). HRMS (ESI) calculated for $C_6H_7N_2S_2$ $[M + H]^+$ m/z 170.2480, found 170.2482.

*4.2.2. Preparation of ethyl 3-amino-4-cyano-5-(methylthio)thiophene-2-carboxylate(**2**)*

At 0 °C, 2-(Bis(Methylthio)methylene)malononitrile **1** (15.0 g, 88.2 mmol) was added to a solution of ethyl 2-mercaptoacetate (9.8 mL, 88.2 mmol) in EtOH (75 mL), then Et_3N (12.2 mL, 88.2 mmol) was added dropwise to the solution and stirred for 12 h at 20 °C. The reaction mixture was filtered, washed with EtOH (20 mL) and dried under reduced pressure to afford product **2** as a

white solid (15.5 g, 72.6%). ^{1}H NMR (400 MHz, $CDCl_3$) δ 5.79 (s, 2H). 4.28 (q, *J* = 7.2 Hz, 2H) 2.64 (s, 3H) 1.34 (t, *J* = 7.1 Hz, 3H). HRMS (ESI) calculated for $C_9H_{11}N_2O_2S_2$ $[M + H]^+$ m/z 243.0264, found 243.0266.

*4.2.3. Preparation of ethyl 4-cyano-3-iodo-5-(methylthio)thiophene-2-carboxylate(**3**)*

A suspension of ethyl 3-amino-4-cyano-5-(methylthio)thiophene-2-carboxylate **2** (7.5 g, 31.1 mmol) in acetontrile (75 mL) was treated with I_2 (6.0 g, 62.0 mmol) then heated to 70 °C, and isoamyl nitrite (6.3 mL, 62.0 mmol) was added at a rate to maintain the pot temperature between 60 °C and 70 °C. Then the mixture was cooled to 20 °C and stirred for 12 h. Upon cooling to 0 °C, the reaction mixture was filtered, and washed with acetonitrile (10 mL) , the solid was redissolved in 60 mL ethyl acetate, washed with saturated sodium thiosulfate (15 mL×2) and then brine. The organic layer was dried over Na_2SO_4, filtered, and concentrated under reduced pressure and dried under reduced pressure to afford product **3** as a yellow solid (6.9 g, 63.0%). ^{1}H NMR (400 MHz, $CDCl_3$) δ 4.31 (q, *J* = 7.1 Hz, 2H) 2.63 (s, 3H) 1.34 (t, *J* = 7.1 Hz, 3H). HRMS (ESI) calculated for $C_9H_9INO_2S_2$ $[M + H]^+$ m/z 353.9119, found: 353.9110.

*4.2.4. Preparation of ethyl 4-cyano-3-iodo-5-(methylsulfonyl)thiophene-2-carboxylate(**4**)*

30% H_2O_2 (37.5 mL) was added to a solution of ethyl 4-cyano-3-iodo-5-(methylthio)thiophene-2-carboxylate **3** (3.8 g, 10.7 mmol) and sodium tungstate (0.3 g, 1.1 mmol) in acetic acid (75 mL). The mixture was stirred at 60 °C for 2 h. After Cooling to room temperature., the reaction mixture was filtered, washed with H_2O (20 mL) and dried under reduced pressure to afford product **4** as a white solid (3.9 g), which was carried into the next step whithout further purification.

*4.2.5. Preparation of ethyl 4-cyano-3-iodo-5-morpholinothiophene-2-carboxylate(**5**)*

Ethyl 4-cyano-3-iodo-5-(methylsulfonyl)thiophene-2-carboxylate **4** (3.9 g, 10.7 mmol) was added to THF (60 mL), and then the mixture was cooled to 0 °C, morpholine (4.8 mL, 55.1 mmol) was added with pot temperature below 10 °C. The reaction was stirred at 25 °C for 8 h. The reaction mixture was poured into ice-water (30 mL) and the resulting precipitate was filtered and dried under reduced pressure to abtain **5** as a white solid (3.2 g, 75.5%). ^{1}H NMR (400 MHz, $CDCl_3$) δ 4.34 (q, *J* = 7.2 Hz, 2H) 3.96-3.83 (m, 4H), 3.70-3.54 (m, 4H), 1.36 (t, *J* = 7.1 Hz, 3H). HRMS (ESI) calculated for $C_{12}H_{14}IN_2O_3S$ $[M + H]^+$ m/z 392.9770, found: 392.9762.

4.2.6. Preparation of ethyl 3-(4-((tert-butoxycarbonyl)amino)phenyl)-4-cyano-5-morpholin-

*othiophene-2-carboxylate(**6**)*

Ethyl 4-cyano-3-iodo-5-morpholinothiophene-2-carboxylate **5** (2.6 g, 6.6 mmol), 4-(N-Boc-amino)phenylboronic acid pinacol ester (2.2 g, 6.6 mmol), $Pd_2(dba)_3$ (0.18g, 0.2 mmol) and CsF (3.0 g, 19.8 mmol) were added to a solution of 1,4-dioxane and H_2O (30 mL, 1,4-dioxane:H_2O = 4:1). The reactor was flushed with N_2, $P(t\text{-}Bu)_3$ (0.4 mL of a 1M solution in Toluene, 0.4 mmol) was added via syringe to the mixture and stirred for 12 h at 95 °C. Upon completion, Water (30 mL) was added followed by extraction with EtOAc (10 mL×3). The organic layer was decolored with 5% active carbon and then filtered through a Celite pad. The filtrate was concentrated to dryness and then triturated with MeOH to obtain **6** as a white solid (2.4 g, 78.9%). ^{1}H NMR (400 MHz, $CDCl_3$) δ 7.43 (d, *J* = 8.4 Hz, 2H), 7.36 – 7.29 (d, *J* = 8.4 Hz, 2H), 6.59 (s, 1H), 4.14 (q, *J* = 7.1 Hz, 2H), 3.90 – 3.83 (m, 4H), 3.65 – 3.58 (m, 4H), 1.52 (s, 9H), 1.16 (t, *J* = 7.1 Hz, 3H). HRMS (ESI) calculated for $C_{23}H_{28}N_3O_5S$ $[M + H]^+$ m/z 458.1750, found: 458.1751.

*4.2.7. Preparation of 3-(4-((tert-butoxycarbonyl)amino)phenyl)-4-cyano-5-morpholino-thiophene -2-carboxylic acid(**7**)*

A solution of LiOH (1.6 g, 66 mmol) in H_2O (15 mL) was added to a solution of 3-(4-((tert-butoxycarbonyl)amino)phenyl)-4-cyano-5-morpholin-othiophene-2-carboxylate **6** (6.0 g, 13.2 mmol) in MeOH (30 mL) and THF (60 mL). The mixture was stirred for 4 h at 25 °C. The reactor was concentrated under reduced pressure and poured into water (30 mL). The solution was adjusted to pH=5 with 2N HCl, and then the resulting precipitate was filtered, washed with H_2O (20 mL) and a minimal amount of MeOH, dried under reduced pressure to afford product **8** as a white solid (4.4 g, 71.4%). HRMS (ESI) calculated for $C_{21}H_{22}N_3O_5S$ $[M - H]^-$ m/z 430.1437, found: 430.1442.

*4.2.8. Preparation of tert-butyl(4-(2-carbamoyl-4-cyano-5-morpholinothiophen-3-yl)phenyl) carbamate(**8**)*

A suspension of 3-(4-((tert-butoxycarbonyl)amino)phenyl)-4-cyano-5-morpholino-thiophene -2-carboxylic acid **7** (5.4 g, 12.6 mmol) in THF (120 mL) was treated with Et_3N (2.4 mL, 18.9 mmol) in one portion. The reactor was cooled to 0 °C, and methyl chloroformate (1.8 g, 18.9 mmol) was added drop-wise. The mixture was stirred at 25 °C for 3 h and then cooled to 0 °C. $NH_3 \cdot H_2O$ (27 mL) was added to the solution. The reaction was warmed to 25 °C and stirred for 1

h. The mixture was concentrated under reduced pressure and poured into water (50 mL), and the resulting precipitate was filtered, washed with H_2O (20 mL) and dried under reduced pressure to afford product **8** as a yellow solid (4.7 g, 86.1%). ^{1}H NMR (400 MHz, DMSO-d_6) δ 9.61 (s, 1H), 7.59 (d, *J* = 8.7 Hz, 2H), 7.29 (d, *J* = 8.7 Hz, 2H), 3.80 – 3.72 (m, 4H), 3.56 – 3.50 (m, 4H), 1.49 (s, 9H). HRMS (ESI) calculated for $C_{21}H_{25}N_4O_4S$ $[M + H]^+$ m/z 429.1597, found: 429.1603.

*4.2.9. Preparation of tert-butyl (E)-(4-(4-cyano-2-(((dimethylamino)methylene)carbamoyl)-5-morpholinothiophen-3-yl)phenyl)carbamate(**9**)*

DMF-DMA (3.0 g, 25.2 mmol) was added to a stirring solution of tert-butyl (4-(2-carbamoyl-4-cyano-5-morpholinothiophen-3-yl)phenyl)carbamate **8** (5.4 g, 12.6 mmol) in DMF (40 mL) and heated to 110 °C for 2 h. After being cooled to room temperature, the mixture was concentrated under reduced pressure and poured into ice-water (30 mL). The precipitate was filtered, washed with H_2O (10 mL) and MeOH (5 mL), dried under reduced pressure to afford product **9** as a yellow solid (4.4 g, 71.4%). HRMS (ESI) calculated for $C_{24}H_{30}N_5O_4S$ $[M + H]^+$ m/z 484.2019, found: 484.2020.

*4.2.10. Preparation of tert-butyl (4-(4-cyano-5-morpholino-2-(1H-1,2,4-triazol-3-yl)thiophen-3-yl) phenyl)carbamate(**10**)*

80% hydrazine hydrate (15 mL) was added drop-wise to a solution of tert-butyl (E)-(4-(4-cyano-2-(((dimethylamino)methylene)carbamoyl)-5-morpholinothiophen-3-yl)phenyl)ca rbamate **9** (3.0g, 6.2 mmol) in HOAc (30 mL). The mixture was stirred at 60 ℃ for 2 h. Upon cooling to room temperature, the solvent was removed under vacuum, and then H_2O (30 mL) was added to the mixture. The resulting precipitate was filtered and dried under reduced pressure to afford **10** as a white solid (2.4 g, 85.5%). HRMS (ESI) calculated for $C_{22}H_{25}N_6O_3S$ $[M + H]^+$ m/z 453.1709, found: 453.1710.

*4.2.11. Preparation of 4-(4-aminophenyl)-2-morpholino-5-(1H-1,2,4-triazol-3-yl)thiophene-3-carbonitrile(**11**)*

tert-Butyl(4-(4-cyano-5-morpholino-2-(1*H*-1,2,4-triazol-3-yl)thiophen-3yl)phenyl)carbamate **10** (3.0 g, 6.6 mmol) was added to CH_2Cl_2 (60 mL), and then the mixture was cooled to 0 °C, CF_3COOH (3.1 mL, 22.0 mmol) was added to the solution drop-wise. The mixture was stirred at 25 °C for 3 h. The solvent was removed under vacuum, and then H_2O (30 mL) was added to the mixture. The solution was adjusted to pH=8 with Et_3N, and then the resulting precipitate was

filtered and dried under reduced pressure to afford a white solid (1.7 g, 80.0%). ^{1}H NMR (400 MHz, DMSO-d_6) δ 8.37 (s, 1H), 7.04 (d, *J* = 8.4 Hz, 2H), 6.58 – 6.48 (d, *J* = 8.4 Hz, 2H), 5.24 (s, 2H), 3.85 – 3.71 (m, 4H), 3.52 – 3.41 (m, 4H). HRMS (ESI) calculated for $C_{17}H_{17}N_6OS$ $[M + H]^+$ m/z 353.1185, found: 353.1170.

4.3. Synthesis of the target compounds ***12a-m***

4.3.1. General procedure for preparation of the target compounds ***12a-m***

A mixture of different substituted isocyanate (14.0 mmol), CH_2Cl_2 (40 mL) and 4-(4-aminophenyl)-2-morpholino-5-(1H-1,2,4-triazol-3-yl)thiophene-3-carbonitrile **11** (9.3 mmol) was stirred at 25 °C for 12 h. The resulting precipitate was filtered and recrystallization from CH_3CN to afford target products **12a-m**.

*4.3.1.1.1-(4-(4-cyano-5-morpholino-2-(1H-1,2,4-triazol-5-yl)thiophen-3-yl)phenyl)-3-(2,6-dimeth ylphenyl)urea(**12a**)*

White solid; Yield: 70.1%; ^{1}H NMR (400 MHz, DMSO) δ 13.99 (s, 1H), 9.25 (s, 1H), 8.45 (s, 1H), 8.08 (s, 1H), 7.47 (d, *J* = 8.4 Hz, 2H), 7.25 (d, *J* = 8.0 Hz, 2H), 7.11–7.00 (m, 3H), 3.84 – 3.76 (m, 4H), 3.55 – 3.48 (m, 4H). 2.22 (s, 6H). m.p.: 217.8 – 219.3 ^{o}C. HRMS (ESI) calculated for $C_{26}H_{26}N_7O_2S$ $[M + H]^+$ m/z 476.1869, found: 476.1866.

4.3.1.2.

*1-(4-(4-cyano-5-morpholino-2-(1H-1,2,4-triazol-5-yl)thiophen-3-yl)phenyl)-3-(p-tolyl)urea (**12b**)*

White solid; Yield: 67.8%; ^{1}H NMR (400 MHz, DMSO-d_6) δ 13.99 (s, 1H), 8.95 (s, 1H), 8.81 (s, 1H), 8.46 (s, 1H), 7.46 (d, *J* = 8.3 Hz, 2H), 7.35 (d, *J* = 8.3 Hz, 2H), 7.28 (d, *J* = 8.3 Hz, 2H), 7.09 (d, *J* = 8.2 Hz, 2H), 3.84 – 3.74 (m, 4H), 3.55 – 3.48 (m, 4H), 2.24 (s, 3H). ^{13}C NMR (101 MHz, DMSO-d_6) δ 175.0, 166.3, 156.3, 153.0, 144.2, 140.2, 137.5, 131.2 (2C), 130.7, 129.6 (2C), 127.3, 118.8 (2C), 117.9 (2C), 117.1, 116.0, 90.9, 65.8 (2C), 51.0 (2C), 20.8. m.p.: 231.4 – 232.3 ^{o}C. HRMS (ESI) calculated for $C_{25}H_{24}N_7O_2S$ $[M + H]^+$ m/z 486.1712, found: 486.1711.

*4.3.1.3.1-(4-(4-cyano-5-morpholino-2-(1H-1,2,4-triazol-5-yl)thiophen-3-yl)phenyl)-3-(2-methoxyp henyl)urea (**12c**)*

White solid; Yield: 66.2%; ^{1}H NMR (400 MHz, DMSO-d_6) δ 13.98 (s, 1H,), 9.46 (s, 1H), 8.46 (s, 1H), 8.29 (s, 1H), 8.15 (d, *J* = 7.8 Hz, 1H), 7.47 (d, *J* = 8.3 Hz, 2H), 7.29 (d, *J* = 8.1 Hz, 2H), 7.03 (d, *J* = 7.4 Hz, 1H), 6.98–6.93 (m, 1H), 6.90 (t, *J* = 7.7 Hz, 1H), 3.89 (s, 3H), 3.84 – 3.74 (m, 4H), 3.55 – 3.48 (m, 4H). ^{13}C NMR (101 MHz, DMSO-d_6) δ 166.3, 153.8, 152.9, 148.2,

140.3, 130.7 (2C), 129.1, 127.2, 123.6, 123.2, 122.3, 121.0, 118.8, 117.7 (2C), 117.1, 116.1, 111.2, 90.9, 65.8 (2C), 56.2, 51.0 (2C). m.p.: 222.3 – 223.9 °C. HRMS (ESI) calculated for $C_{25}H_{24}N_7O_3S$ $[M + H]^+$ m/z 502.1661, found:502.1655.

*4.3.1.4.1-(4-(4-cyano-5-morpholino-2-(1H-1,2,4-triazol-5-yl)thiophen-3-yl)phenyl)-3-(4-cyanophenyl)urea (**12d**)*

White solid; Yield: 72.5%; ^{1}H NMR (400 MHz, DMSO-d_6) δ 13.99 (s, 1H), 9.31 (s, 1H), 9.02 (s, 1H), 8.47 (s, 1H), 7.74 (d, *J* = 8.8 Hz, 2H), 7.66 (d, *J* = 8.8 Hz, 2H), 7.50 (d, *J* = 8.7 Hz, 2H), 7.32 (d, *J* = 8.2 Hz, 2H), 3.83 – 3.78 (m, 4H), 3.55 – 3.48 (m, 4H). ^{13}C NMR (101 MHz, DMSO-d_6) δ 175.0, 166.2, 152.5, 144.6, 144.3, 139.5, 133.8 (2C), 130.7 (2C), 128.0, 123.6, 123.2, 119.8, 118.5 (2C), 118.3 (2C), 117.1, 103.7, 90.9, 65.8 (2C), 51.0 (2C). m.p.: 198.7 – 200.3 °C. HRMS (ESI) calculated for $C_{25}H_{21}N_8O_2S$ $[M + H]^+$ m/z 497.1508, found: 497.1510.

*4.3.1.5.1-(4-(4-cyano-5-morpholino-2-(1H-1,2,4-triazol-5-yl)thiophen-3-yl)phenyl)-3-(4-(trifluoromethyl)phenyl)urea (**12e**)*

White solid; Yield: 67.8%; ^{1}H NMR (400 MHz, DMSO-d_6) δ 13.98 (s, 1H), 9.19 (s, 1H), 8.95 (s, 1H), 8.47 (s, 1H), 7.71 –7.62 (m, 4H), 7.53 – 7.47 (d, *J* = 8.6 Hz, 2H), 7.32 (d, *J* = 8.3 Hz, 2H), 3.84 – 3.76 (m, 4H), 3.56 – 3.48 (m, 4H). ^{13}C NMR (101 MHz, DMSO-d_6) δ 175.0, 166.2, 152.7, 143.9, 134.0, 130.7 (2C), 126.55 (q, J_{C-F} = 3.6 Hz, 2C), 126.4, 123.7, 123.6, 123.2, 122.2 (q, J_{C-F} = 31.0 Hz, 2C), 118.3 (2C), 118.2, 117.1, 116.0, 90.9, 65.8 (2C), 51.0 (2C). m.p.: 228.5 – 230.1 °C. HRMS (ESI) calculated for $C_{25}H_{21}F_3N_7O_2S$ $[M + H]^+$ m/z 540.1430, found: 540.1432.

*4.3.1.6.1-(4-(4-cyano-5-morpholino-2-(1H-1,2,4-triazol-5-yl)thiophen-3-yl)phenyl)-3-(4-(trifluoromethoxy)phenyl)urea (**12f**)*

White solid; Yield: 66.2%; ^{1}H NMR (400 MHz, DMSO-d_6) δ 13.98 (s, 1H), 9.32 (s 1H), 9.22 (s, 1H), 8.43 (s, 1H), 7.64 – 7.55 (d, *J* = 9.3 Hz, 2H), 7.53 – 7.47 (d, *J* = 8.6 Hz, 2H), 7.35 – 7.25 (m, 4H), 3.85 – 3.76 (m, 4H), 3.55 – 3.48 (m, 4H). ^{13}C NMR (101 MHz, DMSO-d_6) δ 166.3, 153.8, 153.0, 143.0, 140.7, 140.0, 139.6, 130.7 (2C), 127.4, 123.6, 123.2, 122.2 (2C), 120.4 (q, J_{C-F} = 253.5 Hz), 119.7 (2C), 117.9 (2C), 117.1, 90.9, 65.8 (2C), 51.0 (2C). m.p.: 208.8 – 210.1 °C. HRMS (ESI) calculated for $C_{25}H_{21}F_3N_7O_3S$ $[M + H]^+$ m/z 556.1379, found: 556.1385.

*4.3.1.7.1-(4-(4-cyano-5-morpholino-2-(1H-1,2,4-triazol-5-yl)thiophen-3-yl)phenyl)-3-(4-fluorophenyl)urea (**12g**)*

White solid; Yield: 65.9%; ^{1}H NMR (400 MHz, DMSO-d_6) δ 13.99 (s, 1H), 9.17 (s, 1H),

9.07 (s, 1H), 8.46 (s, 1H), 7.58 (d, *J* = 8.9 Hz, 2H), 7.48 (d, *J* = 8.3 Hz, 2H), 7.29 (d, *J* = 8.4 Hz, 4H), 3.84 – 3.76 (m, 4H), 3.55 – 3.48 (m, 4H). ^{13}C NMR (101 MHz, DMSO-d_6) δ 166.2, 159.0, 156.6, 155.0 (d, J_{C-F} = 247.8 Hz), 153.1, 144.3, 140.1, 139.5, 130.7 (2C), 127.5, 123.6, 123.2, 120.4 (d, J_{C-F} = 7.6 Hz, 2C), 118.0 (2C), 117.1, 115.7 (d, J_{C-F} = 22.0 Hz, 2C), 90.9, 65.8 (2C), 51.0 (2C). m.p.: 244.5 – 245.8 °C. HRMS (ESI) calculated for $C_{24}H_{21}FN_7O_2S$ $[M + H]^+$ m/z 490.1461, found:490.1456.

*4.3.1.8.1-(4-(4-cyano-5-morpholino-2-(1H-1,2,4-triazol-5-yl)thiophen-3-yl)phenyl)-3-(2-fluorophenyl)urea (**12h**)*

White solid; Yield: 58.7%; ^{1}H NMR (400 MHz, DMSO-d_6) δ 14.04 (s, 1H), 9.65 (s, 1H), 8.80 (s, 1H), 8.46 (s, 1H), 8.16 (t, *J* = 7.7 Hz, 1H), 7.49 (d, *J* = 8.0 Hz, 2H), 7.30 (d, *J* = 7.9 Hz, 2H), 7.27–7.18 (m, 1H), 7.14 (t, *J* = 7.6 Hz, 1H), 7.08 – 6.95 (m, 1H), 3.83 – 3.76 (m, 4H), 3.55 – 3.48 (m, 4H). m.p.: 244.5 – 245.7 °C. HRMS (ESI) calculated for $C_{24}H_{21}FN_7O_2S$ $[M + H]^+$ m/z 490.1461, found:490.1464.

*4.3.1.9.1-(4-(4-cyano-5-morpholino-2-(1H-1,2,4-triazol-5-yl)thiophen-3-yl)phenyl)-3-(3-fluorophenyl)urea (**12i**)*

White solid; Yield: 81.2%; ^{1}H NMR (400 MHz, DMSO-d_6) ^{1}H NMR (400 MHz, DMSO-d_6) δ 13.98 (s, 1H), 8.99 (s, 1H), 8.88 (s, 1H), 8.46 (s, 1H), 7.54 – 7.45 (m, 3H), 7.33 – 7.25 (m, 3H), 7.16 – 7.12 (m, 1H), 6.82 – 6.75 (m, 1H), 3.83 – 3.76 (m, 4H), 3.55 – 3.48 (m, 4H). ^{13}C NMR (101 MHz, DMSO-d_6) δ 175.0, 162.9 (d, J_{C-F} = 239.2 Hz), 153.8, 152.8 144.3, 142.1, 142.0, 130.8, 130.7 (2C), 123.6, 123.2, 118.1 (2C), 117.1, 116.0, 114.4 (d, J_{C-F} = 2.6 Hz), 108.6 (d, J_{C-F} = 21.3 Hz), 105.3 (d, J_{C-F} = 26.5 Hz)，90.9, 65.8 (2C), 51.0 (2C). m.p.: 223.2 – 225.0 °C. HRMS (ESI) calculated for $C_{24}H_{21}FN_7O_2S$ $[M + H]^+$ m/z 490.1457, found:490.1457.

*4.3.1.10.1-(3-chloro-4-fluorophenyl)-3-(4-(4-cyano-5-morpholino-2-(1H-1,2,4-triazol-5-yl)thiophen-3-yl)phenyl)urea (**12j**)*

White solid; Yield: 72.1%; ^{1}H NMR (400 MHz, DMSO-d_6) δ 14.02 (s, 1H), 9.57 (s, 1H), 9.41 (s, 1H), 8.46 (s, 1H), 7.81 (d, *J* = 7.5 Hz, 1H), 7.47 (d, *J* = 8.4 Hz, 2H), 7.34 (s, 1H), 7.31 (d, *J* = 8.6 Hz, 2H), 7.28 (s, 1H), 3.83 – 3.76 (m, 4H), 3.55 – 3.48 (m, 4H). ^{13}C NMR (101 MHz, DMSO-d_6) δ 174.9, 166.3, 153.8, 152.9, 152.8 (d, J_{C-F} = 247.8 Hz), 151.6, 137.5 (d, J_{C-F} = 2.9 Hz), 134.6, 130.7 (2C), 123.4 (d, J_{C-F} = 44.0 Hz), 120.0 (2C), 119.6 (d, J_{C-F} = 18.2 Hz), 119.0 (d,

J = 6.8 Hz), 118.2, 117.3 (d, J_{C-F} = 36.1 Hz), 117.2, 116.0, 90.9, 65.8 (2C), 51.0 (2C). m.p.: 238.7 – 240.4 °C. HRMS (ESI) calculated for $C_{24}H_{20}ClFN_7O_2S$ $[M + H]^+$ m/z 524.9777, found:524.1204.

*4.3.1.11.1-(2-chlorophenyl)-3-(4-(4-cyano-5-morpholino-2-(1H-1,2,4-triazol-5-yl)thiophen-3-yl)phenyl)urea(**12k**)*

White solid; Yield: 77.1%; ^{1}H NMR (400 MHz, DMSO-d_6) δ 14.03 (s, 1H), 9.84 (s, 1H), 8.49 (s, 1H), 8.46 (s, 1H), 8.17 (d, *J* = 8.2 Hz, 1H), 7.51 (d, *J* = 8.3 Hz, 2H), 7.46 (d, *J* = 8.0 Hz, 1H), 7.32 (s, 1H), 7.29 (d, *J* = 7.0 Hz, 2H), 7.03 (t, *J* = 7.6 Hz, 1H), 3.84 – 3.76 (m, 4H), 3.55 – 3.48 (m, 4H). ^{13}C NMR (101 MHz, DMSO-d_6) δ 166.2, 156.3, 152.6, 144.3, 139.8, 139.4, 136.4, 130.8, 129.7, 128.1 (2C), 127.8, 123.8, 122.5, 121.8, 117.9 (2C), 117.1, 115.0, 90.9, 65.8 (2C), 51.0 (2C). m.p.: 232.5 – 233.7 °C. HRMS (ESI) calculated for $C_{24}H_{21}ClN_7O_2S$ $[M + H]^+$ m/z 506.1166, found: 506.1170.

4.3.1.12.1-(3-bromophenyl)-3-(4-(4-cyano-5-morpholino-2-(1H-1,2,4-triazol-5-yl)thiophen-3-yl)phenyl)urea*(**12l**)*

White solid; Yield: 68.1%; ^{1}H NMR (400 MHz, DMSO-d_6) δ 13.99 (s, 1H), 9.14 (s, 1H), 9.06 (s, 1H), 8.46 (s, 1H), 7.87 (s, 1H), 7.47 (d, *J* = 8.4 Hz, 2H), 7.33 (d, *J* = 8.7 Hz, 1H), 7.30 (d, *J* = 8.3 Hz, 2H), 7.24 (t, *J* = 8.0 Hz, 1H), 7.15 (d, *J* = 7.9 Hz, 1H), 3.84 – 3.76 (m, 4H), 3.55 – 3.48 (m, 4H). m.p.: 245.6 – 247.0 °C. HRMS (ESI) calculated for $C_{24}H_{21}BrN_7O_2S$ $[M + H]^+$ m/z 550.0661, found: 550.0660.

*4.3.1.13.1-(4-(4-cyano-5-morpholino-2-(1H-1,2,4-triazol-5-yl)thiophen-3-yl)phenyl)-3-phenylurea (**12m**)*

White solid; Yield: 62.7%; ^{1}H NMR (400 MHz, DMSO-d_6) δ 14.00 (s, 1H), 9.26 (s, 1H), 9.05 (s, 1H), 8.57 (s, 1H), 7.91 (d, *J* = 8.2 Hz, 2H), 7.58 (d, *J* = 8.3 Hz, 2H), 7.47-7.36 (m, 3H), 7.32 – 7.26 (m, 2H), 3.84 – 3.76 (m, 4H), 3.56 – 3.48 (m, 4H). m.p.: 229.1 – 231.8 °C. HRMS (ESI) calculated for $C_{24}H_{22}N_7O_2S$ $[M + H]^+$ m/z 471.1467, found: 471.1462.

*4.4. Synthesis of the target compounds **15a-o***

*4.4.1. Preparation of phenyl (4-(4-cyano-5-morpholino-2-(1H-1,2,4-triazol-3-yl)thiophen-3-yl) phenyl)carbamate(**13**)*

Phenyl chloroformate (2.3 mL, 18.0 mmol) was added drop-wise to a solution of intermediate **11** (4.2 g, 12.0 mmol) in acetone (80 mL). The mixture was stirred at 25 °C for 3 h. The solvent was evaporated *in vacuo*. The mixture was diluted with CH_2Cl_2 (30 mL) and washed with H_2O (2

× 10 mL). The organic phase was dried with Na_2SO_4 and evaporated *in vacuo* to afford **13** as a white solid (4.1 g, 73.2%). HRMS (ESI) calculated for $C_{24}H_{21}N_6O_3S$ $[M + H]^+$ m/z 473.1318, found: 473.1316.

*4.4.2. Preparation of N-(4-(4-cyano-5-morpholino-2-(1H-1,2,4-triazol-3-yl)thiophen-3-yl)phenyl)hydrazinecarboxamide(**14**)*

80% $NH_2NH_2 \cdot H_2O$ (1.0 mL, 12.0 mmol) was added drop-wise to a solution of intermediate **13** (2.8 g, 6.0 mmol) in 1, 4-dioxane (50 mL). The mixture was stirred at 100 °C for 2 h. The resulting precipitate was filtered and dried under reduced pressure to afford **14** as a white solid (2.1 g, 85.3%). HRMS (ESI) calculated for $C_{18}H_{19}N_8O_2S$ $[M + H]^+$ m/z 411.1273, found: 411.1276.

*4.4.3. General procedure for preparation of the target compounds **15a-m***

A mixture of intermediate **14** (5.0 mmol) and different substituted aldehydes (6.0 mmol) in EtOH (10 mL) and HOAc (1 mL) was stirred at 80 °C for 5 h. Upon cooling to room temperature, the resulting precipitate was filtered, washed with EtOH and dried under reduced pressure to afford target products **15a-m**.

*4.4.3.1(E)-2-benzylidene-N-(4-(4-cyano-5-morpholino-2-(1H-1,2,4-triazol-3-yl)thiophen-3-yl)phenyl)hydrazine-1-carboxamide (**15a**)*

White solid; Yield: 64.5%; ^{1}H NMR (400 MHz, DMSO-d_6) δ 14.00 (s, 1H), 10.80 (s, 1H), 9.03 (s, 1H), 8.46 (s, 1H), 7.97 (s, 1H), 7.86 (d, *J* = 6.9 Hz, 2H), 7.68 (d, *J* = 8.3 Hz, 2H), 7.47-7.36 (m, 3H), 7.32 (d, *J* = 8.1 Hz, 2H), 3.84 – 3.76 (m, 4H), 3.56 – 3.48 (m, 4H). ^{13}C NMR(101MHz, DMSO-d_6) δ 166.2, 156.3, 153.5, 144.3, 141.4, 139.5, 139.4, 134.8 (2C), 130.4, 129.9 (2C), 129.1, 128.2, 127.5 (2C), 119.7 (2C), 117.1, 114.9, 90.8, 65.7 (2C), 51.0 (2C). m.p.: 241.8 – 243.6 ^{o}C. HRMS (ESI) calculated for $C_{25}H_{23}N_8O_2S$ $[M + H]^+$ m/z 499.1665, found: 499.1659.

*4.4.3.2. (E)-N-(4-(4-cyano-5-morpholino-2-(1H-1,2,4-triazol-3-yl)thiophen-3-yl)phenyl)-2-(4-fluorobenzylidene)hydrazine-1-carboxamide (**15b**)*

White solid; Yield: 74.2%; ^{1}H NMR (400 MHz, DMSO-d_6) δ 13.99 (s, 1H), 10.90 (s, 1H), 9.08 (s, 1H), 8.47 (s, 1H), 8.02 (s, 1H), 7.99 (s, 2H), 7.66 (d, *J* = 8.3 Hz, 2H), 7.41 (d, *J* = 8.3 Hz, 2H), 7.32 (d, *J* = 8.3 Hz, 2H), 3.84 – 3.76 (m, 4H), 3.56 – 3.48 (m, 4H).^{13}C NMR(101MHz,

DMSO-d_6) δ 166.2, 163.2 (d, J_{C-F} = 247.2 Hz), 156.3, 153.6, 144.3, 140.2, 139.5, 139.5, 139.4, 131.5, 131.4, 130.4 (2C), 129.6 (d, J_{C-F} = 8.2 Hz), 128.2, 119. 8 (2C), 117.1, 116.0 (d, J_{C-F} = 21.7 Hz), 114.9, 90.9, 65.8 (2C), 51.0 (2C). m.p.: 239.1 – 240.7 ^{o}C. HRMS (ESI) calculated for $C_{25}H_{22}FN_8O_2S$ [M + H]$^+$ m/z 517.1570, found: 517.1562.

*4.4.3.3. (E)-N-(4-(4-cyano-5-morpholino-2-(1H-1,2,4-triazol-3-yl)thiophen-3-yl)phenyl)-2-(3-bromobenzylidene)hydrazine-1-carboxamide (**15c**)*

White solid; Yield: 75.2%; ^{1}H NMR (400 MHz, DMSO-d_6) δ 13.99 (s, 1H), 10.91 (s, 1H), 9.14 (s, 1H), 8.45 (s, 1H), 8.18 (s, 1H), 7.93 (s, 1H), 7.78 (d, *J* = 7.8 Hz, 1H), 7.66 (d, *J* = 8.5 Hz, 2H), 7.56 (d, *J* = 8.0 Hz, 1H), 7.38 (t, *J* = 7.8 Hz, 1H), 7.31 (d, *J* = 8.3 Hz, 2H), 3.82 – 3.77 (m, 4H), 3.54 – 3.49 (m, 4H). m.p.: 240.1 – 241.5 ^{o}C. HRMS (ESI) calculated for $C_{25}H_{22}BrN_8O_2S$ [M + H]$^+$ m/z 577.0770, found: 577.0763.

*4.4.3.4. (E)-N-(4-(4-cyano-5-morpholino-2-(1H-1,2,4-triazol-3-yl)thiophen-3-yl)phenyl)-2-(3-hydroxybenzylidene)hydrazine-1-carboxamide (**15d**)*

White solid; Yield: 61.5%; ^{1}H NMR (400 MHz, DMSO-d_6) δ 13.99 (s, 1H), 10.72 (s, 1H), 9.54 (s, 1H), 8.98 (s, 1H), 8.46 (s, 1H), 7.88 (s, 1H), 7.66 (d, *J* = 8.5 Hz, 2H), 7.31 (d, *J* = 8.4 Hz, 2H), 7.27 – 7.19 (m, 3H), 6.81 (d, *J* = 7.4 Hz, 1H), 3.82 – 3.77 (m, 4H), 3.54 – 3.49 (m, 4H). ^{13}C NMR (101MHz, DMSO-d_6) δ 166.2, 158.0, 156.3, 153.5, 144.3, 141.6, 139.5, 136.1, 130.4, 130.1 (2C), 127,5, 119.6, 119.2, 118.7, 117.1 (2C), 114.9, 113.8, 90.9, 65.8 (2C), 51.0 (2C). m.p.: 241.7 – 242.5 ^{o}C. HRMS (ESI) calculated for $C_{25}H_{23}N_8O_3S$ [M + H]$^+$ m/z 515.1614, found: 515.1602.

*4.4.3.5. (E)-N-(4-(4-cyano-5-morpholino-2-(1H-1,2,4-triazol-3-yl)thiophen-3-yl)phenyl)-2-(4-methoxyphenyl)benzylidene)hydrazine-1-carboxamide (**15e**)*

White solid; Yield: 77.3%; ^{1}H NMR (400 MHz, DMSO-d_6) δ 14.00 (s, 1H), 10.67 (s, 1H), 8.98 (s, 1H), 8.47 (s, 1H), 7.92 (s, 1H), 7.80 (d, *J* = 8.7 Hz, 2H), 7.68 (d, *J* = 8.5 Hz, 2H), 7.32 (d, *J* = 8.5 Hz, 2H), 6.99 (d, *J* = 8.8 Hz, 2H), 3.81 (s, 3H), 3.82 – 3.77 (m, 4H), 3.54 – 3.49 (m, 4H). ^{13}C NMR (101MHz, DMSO-d_6) δ 166.2, 160.8, 156.3, 153.6, 144.3, 141.3, 139.5, 130.4 (2C), 129.1 (2C), 128.1, 127.5, 119.6 (2C), 117.1, 114.9, 114.5 (2C), 91.0, 65.8, 55.7 (2C), 51.0 (2C). m.p.: 255.6 – 257.7 ^{o}C. HRMS (ESI) calculated for $C_{26}H_{25}N_8O_3S$ [M + H]$^+$ m/z 529.1770, found: 529.1761.

*4.4.3.6. (E)-N-(4-(4-cyano-5-morpholino-2-(1H-1,2,4-triazol-3-yl)thiophen-3-yl)phenyl)-2-(3,4-dihydroxybenzylidene)hydrazine-1-carboxamide (**15f**)*

White solid; Yield: 77.2%; ^{1}H NMR (400 MHz, DMSO-d_6) δ 13.96 (s, 1H), 10.52 (s, 1H), 9.43 (s, 1H), 9.12 (s, 1H), 8.90 (s, 1H), 8.43 (s, 1H), 7.79 (s, 1H), 7.66 (d, *J* = 8.5 Hz, 2H), 7.30 (d, *J* = 8.5 Hz, 2H), 7.26 (d, *J* = 1.6 Hz, 1H), 7.05 (dd, *J* = 8.2, 1.7 Hz, 1H), 6.77 (d, *J* = 8.1 Hz, 1H), 3.82 – 3.77 (m, 4H), 3.54 – 3.49 (m, 4H). m.p.: 246.8 – 248.5 °C. HRMS (ESI) calculated for $C_{25}H_{23}N_8O_4S$ [M + H]$^+$ m/z 531.1563, found: 531.1556.

*4.4.3.7.(E)-N-(4-(4-cyano-5-morpholino-2-(1H-1,2,4-triazol-5-yl)thiophen-3-yl)phenyl)-2-(4-(trifluoromethoxy)benzylidene)hydrazine-1-carboxamide (**15g**)*

White solid; Yield: 85.5%; ^{1}H NMR (400 MHz, DMSO-d_6) δ 13.99 (s, 1H), 10.90 (s, 1H), 9.08 (s, 1H), 8.46 (s, 1H), 8.01 (d, *J* = 8.8 Hz, 2H), 7.99 (s, 1H), 7.67 (d, *J* = 8.5 Hz, 2H), 7.41 (d, *J* = 8.3 Hz, 2H), 7.32 (d, *J* = 8.3 Hz, 2H), 3.83 – 3.76 (m, 4H), 3.55 – 3.49 (m, 4H). ^{13}C NMR (101MHz, DMSO-d_6) δ 166.2, 165.2, 153.5, 149.3, 144.3, 139.7, 134.3, 133.9, 130.4, 130.1 (2C), 130.0, 129.3 (2C), 121.6 (2C), 121.3, 120.5 (q, J_{C-F} = 256.4 Hz), 119.8 (2C), 117.1, 115.0, 91.0, 65.8 (2C), 51.0 (2C). m.p.: 254.6 – 256.3 °C. HRMS (ESI) calculated for $C_{26}H_{22}F_3N_8O_3S$ [M + H]$^+$ m/z 583.1488, found: 583.1481.

*4.4.3.8.(E)-N-(4-(4-cyano-5-morpholino-2-(1H-1,2,4-triazol-5-yl)thiophen-3-yl)phenyl)-2-(2,6-dichlorobenzylidene)hydrazine-1-carboxamide (**15h**)*

White solid; Yield: 76.5%; ^{1}H NMR (400 MHz, DMSO-d_6) δ 13.98 (s, 1H), 11.16 (s, 1H), 8.79 (s, 1H), 8.45 (s, 1H), 8.19 (s, 1H), 7.59 (t, *J* = 8.1 Hz, 4H), 7.43 (t, *J* = 8.1 Hz, 1H), 7.29 (d, *J* = 8.2 Hz, 2H), 3.83 – 3.76 (m, 4H), 3.55 – 3.49 (m, 4H). ^{13}C NMR (101MHz, DMSO-d_6) δ 166.2, 156.3, 153.1, 152.1, 144.3, 139.4, 139.1, 136.1, 134.4 (2C), 131.3, 130.6 (2C), 129.7, 129.4, 128.3, 119.0 (2C), 117.1, 115.0, 90.9, 65.8 (2C), 51.0 (2C). m.p.: 269.7 – 271.4 °C. HRMS (ESI) calculated for $C_{25}H_{21}Cl_2N_8O_2S$ [M + H]$^+$ m/z 567.0885, found: 567.0879.

*4.4.3.9.(E)-N-(4-(4-cyano-5-morpholino-2-(1H-1,2,4-triazol-5-yl)thiophen-3-yl)phenyl)-2-(4-hydroxy-3,5-dimethylbenzylidene)hydrazine-1-carboxamide (**15i**)*

White solid; Yield: 82.4%; ^{1}H NMR (400 MHz, DMSO-d_6) δ 13.99 (s, 1H), 10.55 (s, 1H), 8.90 (s, 1H), 8.63 (s, 1H), 8.47 (s, 1H), 7.81 (s, 1H), 7.68 (d, *J* = 8.5 Hz, 2H), 7.41 (s, 2H), 7.31 (d, *J* = 8.5 Hz, 2H), 3.83 – 3.76 (m, 4H), 3.55 – 3.49 (m, 4H), 2.20(s, 6H). ^{13}C NMR (101MHz, DMSO-d_6) δ 166.2, 156.3, 152.1, 144.3, 139.4, 139.1 (2C), 134.4 (2C), 131.3, 130.6 (2C), 129.7 (2C), 129.4, 128.3, 119.1 (2C), 117.1, 115.0, 90.9, 65.8 (2C), 51.0 (2C). m.p.: 258.7 – 260.1 °C. HRMS (ESI) calculated for $C_{27}H_{27}N_8O_3S$ [M + H]$^+$ m/z 543.1927, found: 543.1920.

*4.4.3.10.(E)-N-(4-(4-cyano-5-morpholino-2-(1H-1,2,4-triazol-5-yl)thiophen-3-yl)phenyl)-2-(3,4,5-trimethoxybenzylidene)hydrazine-1-carboxamide (**15j**)*

White solid; Yield: 77.9%; ^{1}H NMR (400 MHz, DMSO-d_6) δ 13.98 (s, 1H), 10.81 (s, 1H), 9.04 (s, 1H), 8.47 (s, 1H), 7.89 (s, 1H), 7.66 (d, *J* = 8.5 Hz, 2H), 7.32 (d, *J* = 8.5 Hz, 2H), 7.15 (s, 2H), 3.86 (s, 6H), 3.83 – 3.76 (m, 4H), 3.70 (s, 3H), 3.55 – 3.49 (m, 4H). ^{13}C NMR (101MHz, DMSO-d_6) δ 166.2, 156.3, 153.6 (2C), 144.3, 141.3, 139.5, 139.4 (2C), 139.2, 130.5, 130.4 (2C), 128.2, 119.8 (2C), 117.1, 115.0, 104.9, 91.0, 65.8, 60.6 (3C), 56.5 (2C), 51.0 (2C). m.p.: 274.0 – 275.9 ^{o}C. HRMS (ESI) calculated for $C_{28}H_{29}N_8O_5S$ $[M + H]^+$ m/z 589.1982, found: 589.1976.

*4.4.3.11.(E)-2-((1H-pyrrol-2-yl)methylene)-N-(4-(4-cyano-5-morpholino-2-(1H-1,2,4-triazol-5-yl)thiophen-3-yl)phenyl)hydrazine-1-carboxamide (**15k**)*

White solid; Yield: 59.2%; ^{1}H NMR (400 MHz, DMSO-d_6) δ 14.00 (s, 1H), 11.51 (s, 1H), 10.56 (s, 1H), 9.03 (s, 1H), 8.47 (s, 1H), 7.76 (s, 1H), 7.63 (d, *J* = 8.4 Hz, 2H), 7.33 (d, *J* = 8.4 Hz, 2H), 7.01 (s, 1H), 6.38 (s, 1H), 6.12 (dd, *J* = 5.4, 2.4 Hz, 1H), 3.83 – 3.76 (m, 4H), 3.55 – 3.49 (m, 4H). ^{13}C NMR (101MHz, DMSO-d_6) δ 166.3, 165.2, 153.6, 139.6, 134.0, 133.3, 130.5 (2C), 130.1, 130.0, 128.2, 121.7, 117.2, 119.3 (2C), 112.4, 109.5, 70.2, 65.8, 63.3 (2C), 51.0 (2C). m.p.: 258.1 – 259.9 ^{o}C. HRMS (ESI) calculated for $C_{23}H_{22}N_9O_2S$ $[M + H]^+$ m/z 488.1617, found: 488.1611.

*4.4.3.12.(E)-N-(4-(4-cyano-5-morpholino-2-(1H-1,2,4-triazol-5-yl)thiophen-3-yl)phenyl)-2-(furan-2-ylmethylene)hydrazine-1-carboxamide (**15l**)*

White solid; Yield: 66.8%; ^{1}H NMR (400 MHz, DMSO-d_6) δ 14.01 (s, 1H), 10.76 (s, 1H), 8.81 (s, 1H), 8.46 (s, 1H), 8.18 (s, 1H), 7.63 (d, *J* = 5.0 Hz, 1H), 7.61 (d, *J* = 8.2 Hz, 2H), 7.44 (d, *J* = 3.1 Hz, 1H), 7.30 (d, *J* = 7.7 Hz, 2H), 7.12 (dd, *J* = 4.9, 3.7 Hz, 1H), 3.83 – 3.76 (m, 4H), 3.54 – 3.48 (m, 4H). ^{13}C NMR (101MHz, DMSO-d_6) δ 166.2, 156.3, 153.3, 150.1, 144.9, 144.3, 139.4, 139.3, 131.8 (2C), 130.5, 128.1, 119.3, 117.1, 115.0, 112.6 (2C), 112.2, 91.0, 65.8 (2C), 51.0 (2C). m.p.: 247.4 – 249.1 ^{o}C. HRMS (ESI) calculated for $C_{23}H_{21}N_8O_3S$ $[M + H]^+$ m/z 489.1457, found: 489.1448.

*4.4.3.13.(E)-N-(4-(4-cyano-5-morpholino-2-(1H-1,2,4-triazol-5-yl)thiophen-3-yl)phenyl)-2-(pyridin-2-ylmethylene)hydrazine-1-carboxamide (**15m**)*

White solid; Yield: 59.2%; ^{1}H NMR (400 MHz, DMSO-d_6) 13.99 (s, 1H), 10.97 (s, 1H), 9.10 (s, 1H), 9.01 (s, 1H), 8.57 (d, *J* = 3.8 Hz, 1H), 8.47 (s, 1H), 8.32 (d, *J* = 7.9 Hz, 1H), 7.99 (s, 1H), 7.67 (d, *J* = 8.4 Hz, 2H), 7.45 (dd, *J* = 7.8, 4.8 Hz, 1H), 7.32 (d, *J* = 8.4 Hz, 2H), 3.83 – 3.76 (m,

4H), 3.54 – 3.48 (m, 4H). m.p.: 245.8 – 247.2 ^{o}C. HRMS (ESI) calculated for $C_{24}H_{22}N_9O_2S$ [M + H]$^{+}$ m/z 500.1617, found: 500.1598.

4.5. Pharmacology

4.5.1. In vitro enzymatic assays

The in vitro enzymatic assays of target compounds on PI3Ks were evaluated by Kinase-Glo™ assay and ADP-Glo™ Kinase Assay. Briefly, the compound, PI3K enzyme (PI3Kα from Invitrogen, PIK3Cβ from Millipore, PIK3Cγ from Invitrogen, and PIK3Cδ from Millipore), the PIP2 (Life) substrate, and ATP (25 μM, Sigma) were diluted in kinase buffer to the indicated concentrations. The assay plate was covered and incubated at room temperature (PI3Kα, PI3Kβ, and PI3Kγ for 1 h and PI3Kδ for 2 h). Then, the Kinase-Glo reagent (Promega) was added to the PI3Kα plate to stop the reaction and shaken for 15 min. For the PI3Kδ, PI3Kβ, and PI3Kγ inhibition assay, ADP-Glo reagent 1(Promega) was added and shaken slowly for 40 min, followed by the addition of ADP-Glo reagent 2 (Promega), shaken for 1 min, and equilibrated for 60 min, while mTOR inhibition of compound were evaluated by Lance Ultra Assay. Briefly, mTOR enzyme (from Millipore), the ULight-4E-BP1 (Thr37/46) Peptide (Promega), and ATP (13 μM, Sigma) were diluted in kinase buffer to the indicated concentrations. The assay plate was covered and incubated at room temperature for 1h. Then, the detection solution of kinase quench buffer (EDTA, Sigma) and Eu-anti-phospho-4E-BP1 (Promega) was added to the plate to stop the reaction, shaken for 15 min and equilibrated for 60 min. The data were collected on Envision and presented in Excel. IC_{50} values were calculated from the inhibition curves.

4.5.2. Cell proliferation assays

All target compounds were evaluated for antiproliferative potency against U87MG, T47D, H1975, H460 and A549 tumor cell lines using a CellTiter-Glo® Luminescent Cell Viability Assay. The human tumor cell lines used were obtained from the ATCC. All the mediums and FBS were Gibco. T47D, H1975 and H460 tumor cells were cultured in RPMI1640 medium supplemented with 10% FBS. U87MG were cultured in DMEM medium supplemented with 10%FBS. A549 were cultured in Ham's F12K medium supplemented with 10%FBS. The day before treatment with compounds, cells were seeded at a density of 3×10^3 in each well of a 96-well plate. The

tumor cells were then treated with 3-fold serial diluted compound or DMSO control in the incubator at 37 °C and 5% CO_2 for 3 days, prior to the addition of CellTiter-Glo reagents (Promega) and reading of luminescence using a PerkinElmer Envision plate reader. IC_{50} values were determined by curve fitting using XLfit program of Excel software (Microsoft, USA).

4.5.3. Kinase Competition Binding Assays

KINOMEscan competition binding assays (www.kinomescan.com) were performed as described previously.[27] Kinases were produced displayed on T7 phage or by expression in HEK-293 cells and tagged with DNA. Binding reactions were performed at rt for 1 h, and the fraction of kinase not bound to test compound was determined by capture with an immobilized affinity ligand and quantitation by quantitative PCR. Each kinase was tested individually against each compound.

4.5.4. Western Blot Analysis

Cells were treated with **12k** and **PF-4989216** at the indicated concentrations for 2 h at 37 °C before stimulated with 1 μg/mL insulin for 2 h, then the cells were harvested, washed in ice-cold PBS, and lysed with RIPA bu□er, protease inhibitors, phosphatase cocktails A and B, and PMSF (1 mM). Protein concentration was determined by the BCA Kit. The samples were subjected to SDS− PAGE and then transferred onto PVDF membranes (Millpore). The membranes were incubated overnight at 4 °C with the primary antibody (anti-AKT(CST#4691T), anti-$pAKT^{ser473}$ (CST#4060T)in 5% BSA/TBST bu□er with gentle shaking, then washed with 1 × TBS/T 3 times, followed by incubation with secondary antibodies (IRDye 680RD Goat anti-Rabbit antibody; from Licor, Cat. No. 926-68021, 1:10000 dilution), diluted in PBST, for 1 hour at RT. The target blots were detected with Li-Cor Odyssey imager system.

4.5.5. Caco-2 permeability assay

Caco-2 cells purchased from ATCC were seeded onto polyethylene membranes (PET) in 96-well Insert plates at 1 x 10^5 cells/ cm^2, and refreshed medium every 4~5 days until to the 21st to 28th day for confluent cell monolayer formation. Test compound was tested at 2 μM bi-directionally in duplicate. Digoxin was tested at 10 μM bi-directionally in duplicate, while nadolol and metoprolol were tested at 2 μM in A to B direction in duplicate. Final DMSO

concentration was adjusted to less than 1%. The plate was incubated for 2 hours in CO_2 incubator at 37±1°C, with 5% CO_2 at saturated humidity without shaking. And all samples after mixed with acetonitrile containing internal standard were centrifuged at 3200×g for 10 min. Subsequently,100 μL supernatant solution was diluted with 100 μL distilled water for LC/MS/MS analysis. Concentrations of test and control compounds in starting solution, donor solution, and receiver solution were quantified by LC/MS/MS methodologies, using peak area ratio of analyte/internal standard. After transport assay, lucifer yellow rejection assay was applied to determine the Caco-2 cell monolayer integrity. The apparent permeability coefficient Papp (cm/s) was calculated using the equation: Papp = (dCr/dt) x Vr / (A x C_0) .Where dCr/dt is the cumulative concentration of compound in the receiver chamber as a function of time (μM/s); Vr is the solution volume in the receiver chamber (0.075 mL on the apical side, 0.25 mL on the basolateral side); A is the surface area for the transport, C_0 is the initial concentration in the donor chamber (μM). The efflux ratio was calculated using the equation: Efflux Ratio = Papp (B-A) / Papp (A-B)

4.5.6. Liver Microsomal Stability Assay

Two parallel determinations in microsomes, with and without the NADPH regenerating system, were performed for selected compounds. Briefly, the compounds were preincubated with microsomes (human microsome, CORNING Gentest, lot No. 7331001; rat microsome, Xenotech, Lot No. 1310030) (0.5 mg/mL) at 1 μM for 10 min at 37 °C in potassium phosphate buffer (100 mM at pH 7.4 with 10 mM $MgCl_2$). The reactions were initiated by adding prewarmed cofactors (1 mmol NADPH). After incubation for different times (0, 5, 10, 20, 30, and 60 min) at 37 °C, cold acetonitrile was added to precipitate the protein. Then, the samples were centrifuged, and the supernatants were analyzed by LC−MS/MS.

4.5.7. Cytochrome P450 Inhibition Assay

Cytochrome P450 inhibition was evaluated in human liver microsomes (0.25 mg/mL) using three specific probe substrates (CYP1A2, 10 μM phenacetin; CYP2D6, 5μM dextromethorphan; and CYP3A4, 2 μM midazolam) in the presence of multiple concentrations of the test compound 10 μM). After preincubation at 37 °C for 10 min, the reaction was initiated by the addition of 20 μL of NADPH to a final concentration of 10 mM. The mixture was incubated at 37 °C for 10 min,

and the reaction was terminated by the addition of 400 μL of cold stop solution (200 ng/mL tolbutamide and 200 ng/mL labetalol in acetonitrile). After the reactions were terminated, the plates were centrifuged, and the supernatants were analyzed by LC−MS/MS.

4.5.8. In vivo pharmacokinetics

Formulations of compound **12k** were administered intravenously via gavage to Sprague-Dawley rats in full compliance with the Guide for the Care and Use of Laboratory Animals. After intravenous injection with the compound (5 mg/kg), blood samples were collected in heparin-containing tubes at predetermined time points (0.083, 0.25, 0.5, 1, 2, 4, 6, 8, 12 and 24 h) and centrifuged immediately at 4 °C and 4000 rpm for 20 min. Noncompartmental pharmacokinetic parameters were fitted using DAS2.0 based on the LC−MS/MS quantitation data.

4.5.9. hERG QPatch Assay

The CHO-hERG stable cell line used in these experiments was obtained from Sophion Bioscience, Denmark. hERG currents were recorded at room temperature on the Sophion Qpatch 48 HTX (Sophion Biosciences). All experiments were performed in single-hole mode. The cells were voltage clamped at a holding potential of 80 mV. The hERG current was activated by depolarizing at +20 mV for 5 sec, after which the current was taken back to 50 mV for 5 sec to remove the inactivation and observe the deactivating tail current. The K^+ tail current through HERG channels observed during this step was allowed to stabilize under continuous bath perfusion. Cells were then superfused with drug until steady state block was achieved. Steady state was considered reached when three consecutive super-imposable current records were collected. At this point, cells were once again superfused with extracellular solution until the current amplitude returned to values close to those measured before application of drug. More concentrations of drugs were tested on each cell with washout in between each drug application. Cisapride was used in the experiments to ensure the normal response and good quality of the hERG cells.

4.5.10. Molecular docking

The protein coordinates (PDB: 3ZIM; 2Y3A; 3DBS; 2WXP), downloaded from the Protein Data

Bank (http://www.rcsb.org/pdb/), were chosen as templates to compare the docking mode among **12k** bound to PI3Kα, PI3Kβ, PI3Kγ and PI3Kδ. Molecular docking calculations were conducted using the Dock6 protocol in Yinfo Cloud Platform (http://cloud.yinfotek.com/). The structure of compound was built with energy minimization in MMFF94 force field, and PI3Ks was assigned hydrogen atoms and partial charges in Amber ff14SB force field and partial charges in Chimera. The binding pocket of the crystal ligand was assumed to be analogous to that of **12k** in PI3Ks. The box center and the dimensions were thus set. The DOCK 6.7 program was utilized to conduct semiflexible docking with 10 000 different orientations generated. Then, the Grid-based score was calculated for each pose. The image files were generated by Pymol.

Acknowledgements

This work was supported by National Natural Science Foundation of China (No. 81573296, 81903472), LiaoNing Revitalization Talents Program（XLYC1805014), National-Local Joint Engineering Research Center for Innovative & Generic Chemical Drug, Guizhou High-level Innovative Talents Supporting Program (2016-4015). We would also like to thank Guangzhou Yinfo Information Technology Co., Ltd. for providing a friendly and versatile web server (https://cloud.yinfotek.com) to aid the docking studies.

References

[1] I. Vivanco, C. L. Sawyers, The phosphatidylinositol 3-Kinase AKT pathway in human cancer. Nat. Rev. Cancer, 2002, 2: 489-501.

[2] L. M. Thorpe, H. Yuzugullu, J. J. Zhao, PI3K in cancer: divergent roles of isoforms, modes of activation and therapeutic targeting. Nat. Rev. Cancer, 2015, 15(1): 7-24.

[3] P. Liu, H. Cheng, T. M. Roberts, J. J. Zhao, Targeting the phosphoinositide 3-kinase pathway in cancer. Nat. Rev. Drug Discov., 2009, 8(8): 627-644.

[4] B. Vanhaesebroeck, J. Guillermetguibert, M. Graupera, B. Bilanges, The emerging mechanisms of isoform-specific PI3K signalling. Nat. Rev. Mol. Cell Biol., 2010, 11(5): 329-341.

[5] J. A. Engelman, J. Luo, L. C. Cantley, The evolution of phosphatidylinositol 3-kinases as regulators of growth and metabolism. Nat. Rev. Genet., 2006, 7(8): 606-619.

[6] M. Cully, H. You, A. J. Levine, T. W. Mak, Beyond PTEN mutations: the PI3K pathway as an integrator of

multiple inputs during tumorigenesis. Nat. Rev. Cancer, 2006, 6(3): 184-192.

[7] K. Okkenhaug, B. Vanhaesebroeck, PI3K in lymphocyte development, differentiation and activation. Nat. Rev. Immunol., 2003, 3(4): 317-330.

[8] J. Rodon, R. Dienstmann, V. Serra, J. Tabernero, Development of PI3K inhibitors: lessons learned from early clinical trials. Nat. Rev. Clin. Oncol., 2013, 10(3): 143-153.

[9] L. Zhao, P. K. Vogt, Class I PI3K in oncogenic cellular transformation. Oncogene, 2008, 27(41): 5486-5496.

[10] M. Nacht, L. Qiao, M. P. Sheets, T. S. Martin, M. Labenski, H. Mazdiyasni, R. Karp, Z. Zhu, P. Chaturvedi, D. Bhavsar, D. Niu, W. Westlin, R. C. Petter, A.P. Medikonda, J. Singh, Discovery of a potent and isoform-selective targeted covalent inhibitor of the lipid kinase PI3Kα. J. Med. Chem., 2013, 56(3): 712-721.

[11] S. P. Jackson, S. M. Schoenwaelder, I. Goncalves, W. S. Nesbitt, C. L. Yap, C. E. Wright, V. Kenche, K. E. Anderson, S. M. Dopheide, Y. Yuan, S. A. Sturgeon, H. Prabaharan, P. E. Thomspon, G. D. Smith, P. R. Shepherd, N. Daniele, S. Kulkarni, B. Abbott, D. Saylik, C. Jones, L. Lu, S. Giuliano, S. C. Hughan, J. A. Angus, A. D. Robertson, H. H. Salem, PI3-kinase p110beta: a new target for antithrombotic therapy. Nat. Med., 2005, 11(5): 507-514.

[12] K. Okkenhaug, B. Vanhaesebroeck, PI3K in lymphocyte development, differentiation and activation. Nat. Rev. Immunol., 2003, 3(4): 317-330.

[13] T. Ruckle, M. K. Schwarz, C. Rommel, PI3K gamma inhibition: towards an “aspirin of the 21st century”. Nat. Rev. Drug Discov., 2006, 5(11): 903-918.

[14] R. Morrison, T. Belz, S. K. Ihmaid, J. M. A. Al-Rawi, M. J. Angove, Dual and/or selective DNA-PK, PI3K inhibition and isoform selectivity of some new and known 2-amino-substituted-1,3-benzoxazines and substituted-1,3-naphthoxazines. Med. Chem. Res., 2014, 23(11): 4680-4691.

[15] B. J. Lannutti, S. A. Meadows, S. E. M. Herman, A. Kashishian, B. H. Steiner, A. J. Johnson, J. Byrd, J.W. Tyner, M. M. Loriaux, M. Deininger, B. J. Druker, K. D. Puri, R. G. Ulrich, N. Giese, CAL-101, a p110δ selective phosphatidylinositol-3-kinase inhibitor for the treatment of B-cell malignancies, inhibits PI3K signaling and cellular viability. Blood, 2011, 117(2): 591-594.

[16] C. Fritsch, A. Huang, C. Chatenay-Rivauday, C. Schnell, A. Reddy, M. Liu, A. Kauffmann, D. Guthy, D. Erdmann, A. D. Pover, P. Furet, H. Gao, S. Ferretti, Y. Wang, J. Trappe, S. M. Brachmann, S. M. Maira, C. Wilson, M. Boehm, C. Garcia-Echeverria, P. Chene, M. Wiesmann, R. Cotzens, J. Lehar, R. Schlegel, G. Caravatti, F. Hofmann, W. R. Sellers, Characterization of the novel and specific PI3Kα inhibitor

NVP-BYL719 and development of the patient stratification strategy for clinical trials. Mol. Cancer Ther., 2014, 13(5): 1117-1129.

[17] P. Furet, V. Guagnano, R. A. Fairhurst, P. Imbach-Weese, I. Bruce, M. Knapp, C. Fritsch, F. Blasco, J. Blanz, R. Aichholz, J. Hamon, D. Fabbro, G. Caravatti, Discovery of NVP-BYL719 a potent and selective phosphatidylinositol-3 kinase alpha inhibitor selected for clinical evaluation. Bioorg. Med. Chem. Lett., 2013, 23(13): 3741-3748.

[18] K. C. Liu, J. J. Zhu , G. L. Smith, M. J. Yin, S. Bailey, J. H. Chen, Q. Hu, Q. Huang, C. Li, Q. J. Li, M. A. Marx, G. Paderes, P. F. Richardson, N. W. Sach, M. Walls, P. A. Wells, S. Baxi, A. Zou, Highly Selective and Potent Thiophenes as PI3K Inhibitors with Oral Antitumor Activity. ACS Med. Chem. Lett., 2011, 2(11): 809-813.

[19] Z. Zumsteg, N. Morse, G. Krigsfeld, G. Gupta, D. S. Higginson, N. Y. Lee, L. Morris, I. Ganly, S. L. Shiao, S. N. Powell, C. H. Chung, M. Scaltriti, J. Baselga, Taselisib (GDC-0032), a Potent β-sparing Small Molecule Inhibitor of PI3K, Radiosensitizes Head and Neck Squamous Carcinomas Containing Activating PIK3CA Alterations. Clin. Cancer Res., 2015, 22(8): 2009-2019.

[20] S. T. Staben, N. Blaquiere, V. Tsui, A. Kolenikov, S. Do, E. K. Bradley, J. Dotson, R. Goldsmith, T. P. Heffron, J. Lesnick, C. Lewis, J. Murray, J. Nonomiya, A. G. Olivero, J. Pang, L. Rouge, L. Salphati, B. Wei, C. Wiesmann, P. Wu, Cis -Amide isosteric replacement in thienobenzoxepin inhibitors of PI3-kinase. Bioorg. Med. Chem. Lett., 2013, 23(3): 897-901.

[21] B. Barlaam, S. Cosulich, S. Degorce, M. Fitzek, S. Green, U. Hancox, C. L. Brempt, J. J. Lohmann, M. Maudet, R. Morgentin, M. J. Pasquet, A. Peru, P. Ple, T. Saleh, M. Vautier, M. Walker, L. Ward, N. Warin, Discovery of (R)-8-(1-(3,5-difluorophenylamino)ethyl)-*N*,*N*-dimethyl-2-morpholino-4-oxo-4*H*-chromene-6-carboxamide (AZD8186): a potent and selective inhibitor of PI3Kβ and PI3Kδ for the treatment of PTEN-deficient cancers. J. Med. Chem., 2015, 58(2): 943-962.

[22] M. Nacht, L. Qiao, M. P. Sheets, T. S. Martin, M. Labenski, H. Mazdiyasni, R. Karp, Z. Zhu, P. Chaturvedi, D. Bhavsar, D. Niu, W. Westlin, R. C. Petter, A.P. Medikonda, J. Singh, Discovery of a potent and isoform-selective targeted covalent inhibitor of the lipid kinase PI3Kα. J Med Chem., 2013, 56(3): 712-721.

[23] P. Zhan, Y. Itoh, T. Suzuki, X. Y. Liu, Strategies for the Discovery of Target-Specific or Isoform-Selective Modulators. J. Med. Chem., 2015, 58(19): 7611-7633.

[24] Z. Liu, S. Wu, Y. Wang, R. Li, J. Wang, L. Wang, Y. Zhao, P. Gong, Design, synthesis and biological

evaluation of novel thieno[3,2 -d]pyrimidine derivatives possessing diaryl semicarbazone scaffolds as potent antitumor agents. Eur. J. Med. Chem., 2014, 87: 782-793.

[25] Z. Liu, Y. Wang, H. Lin, D. Zuo, L. Wang, Y. Zhao, P. Gong, Design, synthesis and biological evaluation of novel thieno[3,2-d]pyrimidine derivatives containing diaryl urea moiety as potent antitumor agents. Eur. J. Med. Chem., 2014, 85: 215-227.

[26] Q. Huang, P. F. Richardson, N. W. Sach, J. Zhu, K. K. C. Liu, G. L. Smith, D. M. Bowles, Development of Scalable Syntheses of Selective PI3K inhibitors. Org. Process Res. Dev., 2011, 15(3): 556-564.

[27] M. W. Karaman, S. Herrgard, D. K. Treiber, P. Gallant, C. E. Atteridge, B. T. Campbell, K. W. Chan, P. Ciceri, M. I. Davis, P. T. Edeen, R. Faraoni, M. Floyd, J. P. Hunt, D. J. Lockhart, Z. V. Milanov, M. J. Morrison, G. Pallares, H. K. Patel, S. Pritchard, L. M. Wodicka, P. P Zarrinkar. A qualitative analysis of kinase inhibitor selectivity. Nat. Biotechnol., 2008, 26(1), 127– 132.

Highlights

1. Two series of novel 2,3,4,5-tetra-substituted thiophene derivatives containing diaryl urea or N-Acylarylhydrazone scaffold were designed and synthesized as selective PI3Kα inhibitors.
2. Compound **12k** demonstrated nanomolar PI3Kα inhibitory potency with 12, 28, 30, 196-fold selectivity against isoforms β, γ, δ and mTOR.
3. Compound **12k** showed potent antiproliferative activity against T47D, H460, H1975, A549 and U87MG cell lines with IC_{50} values of 0.31μM, 0.20μM, 1.06μM, 3.84μM and 2.86μM, respectively.
4. Compound **12k** showed acceptable profiles in ADME and pharmacokinetic assays.

Declaration of interests

☐ The authors declare that they have no known competing financial interests or personal relationships that could have appeared to influence the work reported in this paper.